

CEBAF PROPOSAL COVER SHEET

This Proposal must be mailed to:

CEBAF
Scientific Director's Office
12000 Jefferson Avenue
Newport News, VA 23606

and received on or before OCTOBER 31, 1989

A. TITLE: Selected studies of the ^3He and ^4He nuclei through electrodisintegration at high momentum transfer

B. CONTACT PERSON: J. MOUGEY

ADDRESS, PHONE AND BITNET:

CEBAF, 12000 Jefferson Ave., Newport News, Va 23606
(804)249-7544 MOUGEY@CEBAFVAX

C. THIS PROPOSAL IS BASED ON A PREVIOUSLY SUBMITTED LETTER OF INTENT

YES
 NO

IF YES, TITLE OF PREVIOUSLY SUBMITTED LETTER OF INTENT

LOI41, LOI51, LOI52, LOI60, LOI89

D. ATTACH A SEPARATE PAGE LISTING ALL COLLABORATION MEMBERS AND THEIR INSTITUTIONS

=====
(CEBAF USE ONLY)

Proposal Received 10-31-89

Log Number Assigned PR-89-044

KES

contact: Mougey

Selected studies of the ^3He and ^4He nuclei through electrodisintegration at high momentum transfer

THE HALL A COLLABORATION

*American University, Cal. State University LA, Case Western Reserve and LANL
Continuous Electron Beam Accelerator Facility*

George Washington University, University of Georgia, Indiana University Cyclotron Facility

Kent State University, University of Maryland, Massachusetts Institute of Technology

University of New Hampshire, National Institute of Science and Technology

Norfolk State University, University of Regina, University of Rochester

University of Saskatchewan, Rutgers University, Stanford University

University of Virginia, University of Washington, College of William and Mary

NIKHEF-K, CEN Saclay, University of Clermont-Ferrand

INFN Sezione Sanita, University of Lund

Spokespersons: M.B. Epstein (Cal. State University LA), R.W. Lourie
(Univ. Virginia), J. Mougey and A. Saha (CEBAF)

We propose to use the CEBAF Hall A High Resolution Spectrometer pair to study selective aspects of the electromagnetic response of ^3He and ^4He through $(e,e'p)$ coincidence measurements at Q^2 values from 0.4 to $4.1(\text{GeV}/c)^2$. In Part I, we propose to study the single nucleon structure of the He isotopes with special emphasis on high momenta (up to $\sim 0.6 \text{ GeV}/c$) by the separation of the R_L , R_T and R_{LT} response functions. The Q^2 dependence of the reaction will be examined in Part II by performing longitudinal/transverse (L/T) separations for protons emitted along \vec{q} , up to $Q^2 = 4.11(\text{GeV}/c)^2$ at quasifree kinematics ($p_m = 0$) and for $Q^2 = 0.5$ and $1.(\text{GeV}/c)^2$ at $p_m = \pm 0.3 \text{ GeV}/c$. In Part III, we focus on the continuum region to study correlated nucleon pairs. Measurements at $Q^2 = 1. (\text{GeV}/c)^2$ and recoil momenta up to $1 \text{ GeV}/c$ are proposed, including separations of the in-plane structure functions for $p_m < 680 \text{ MeV}/c$.

We request a total of 2000 hours of beam time to perform these measurements.

Introduction

During the past twenty years, a wealth of information has been obtained on the single particle aspects of nuclear structure, in particular through elastic, inelastic (e,e') and quasielastic ($e,e'p$) electron scattering experiments. These results have led to strong constraints on the self-consistent mean field description of nuclei, and it is fair to say that the one-body properties of nuclei are now well under control. However, two major issues remain open:

- By increasing the momentum transfer, one is allowed to probe the spatial structure of nuclei over distances comparable or smaller than the nucleon size, where short range correlations between two or several nucleons are important. We must admit that they are poorly known, and their determination is one of the major goals of modern nuclear physics.
- At high momentum transfers, the internal structure of hadrons cannot be ignored. Indeed, the study of the interplay of mesonic and nucleonic degrees of freedom with those of their constituents, using the nucleus as a laboratory, is also a fundamental objective. How a nucleon is affected by the presence of close neighbours in the nuclear medium? Is there a distance where it loses its identity within a large quark cluster?

Coincidence experiments have proven to be very useful tools to study specific aspects of the nucleus. In particular the ($e,e'p$) reaction has been used not only to explore the single nucleon structure of nuclei, but also to study the behavior of nucleons embedded the nuclear medium.

Up to now, both incident energy and duty cycle have been limiting factors in such studies. The high energy, high duty cycle beam of CEBAF will allow to fully develop such studies along the following lines:

- Extend the domain of momentum transfers towards higher values where short-range effects and possibly the internal structure of the nucleons are manifested,
- Explore nuclear structure in its extreme conditions, by focussing on the high momentum part of the wave functions,

- Increase the specificity of the probe by separating the response functions associated with different polarization states of the virtual photon.

We propose to exploit these new possibilities by undertaking a series of $(e,e'p)$ measurements on the Helium isotopes. Next to the deuteron, the $A=3$ and $A=4$ nuclei are the simplest systems in which all of the basic ingredients of a complex nucleus exist. Sophisticated methods to solve the Schrodinger equation almost exactly have been applied to the $A=3$ nuclei and have been extended recently to ${}^4\text{He}$ [1]. Microscopic calculations of FSI and MEC contributions have been developed and applied to reactions on few nucleon systems.[2] For both ${}^3\text{He}$ and ${}^4\text{He}$, a substantial body of coincidence data exists, including accurate measurements of the recoil momentum distribution for the 2-body break-up, up to 400(350) MeV/c in ${}^3\text{He}({}^4\text{He})$. One expect much of the work at $Q^2, 1.(\text{GeV}/c)^2$ to be performed at the existing laboratories, over the next few years. These studies can only be extended into the most interesting high Q^2 regime at CEBAF.

We propose to investigate three specific aspects :

- The structure of the Helium nuclei at high momenta, by separating the various structure functions in perpendicular kinematics.
- The Q^2 dependence of the longitudinal and transverse parts of the $(e,e'p)$ cross section in parallel kinematics.
- A study, in the continuum region, of the electroexcitation of correlated nucleon pairs. This part will also imply the separation of the various responses.

Detection systems and targets

These measurements will be performed in CEBAF Hall A using the High Resolution Spectrometer pair and their associated detection systems. They have been described in details in the CEBAF documents, in particular the PCDR and draft CDR.

Targets for these experiments are being designed currently. These designs call for cryogenic gas targets to be operated at high pressure. Design concerns that have been addressed for these targets have included the high densities required to

achieve luminosities of $10^{38} \text{cm}^{-2} \text{s}^{-1}$, the large amounts of heat deposited by the beam in the target, the high energy densities at the interaction region due to the small size of the beam spot, the containment of density fluctuations due to beam heating and minimizing the thickness of target cell windows.

Preliminary designs for ^3He and ^4He cells specify minimum operating temperature of 10 K and pressure of 70 atm. The corresponding target gas density is 0.17g/cm^3 (for either gas). For a cell of 10 cm (perpendicular) length, luminosities of $(1-4) \times 10^{38} \text{cm}^{-2} \text{s}^{-1}$ can be achieved for beam currents of 50-200 μA . For a cylindrical cell of 15 cm (physical) length with spherical end caps, a wall thickness of 0.03 cm of aluminum 7075-T6 is being incorporated in the current design.

The bulk power dissipation in the target will be dealt with a LHe-4 refrigerator and a suitable heat exchanger. For the ^3He target cell described previously, a maximum power dissipation of 1.2 kW (for a 200 μA beam) is anticipated. To minimize density variations due to local beam heating it is necessary that the target gas flow past the beam. Current preliminary designs specify a gas flow perpendicular to the beam direction at velocities as high as 30 m/s (for ^3He) assuming a tolerable density variation of no more than 20% for a minimum beam spot size of 0.1 mm. Experience in other laboratories, e.g. SLAC, indicates that such velocities are realizable. For a 10% density variation, these velocities are roughly doubled, though they can again be reduced substantially (by more than a factor of two) if the beam is defocused or rastered. For example, it appears that it will be possible for the beam to be defocused to 1-2 mm horizontally which reduces the flow velocities needed by at least a factor of five.

Presently, a collaboration between groups from California State University, Los Angeles and the University of Virginia is involved in the design of these targets in collaboration with a target specialist from SLAC.

Summary of Total Beam Time Request

Part 1 : 340 hours for each nucleus

Part 2 : 250 hours for each nucleus

Part 3 : 300 hours for each nucleus

Setup : 220 hours for setup and calibrations

TOTAL : 2000 hours

Part 1 : Single Nucleon Structure of the He isotopes

1.1. Physics motivation

The choice of perpendicular kinematics is dictated by the physics issues to be investigated. Of special interest in nuclear physics is the study of the high momentum components in nuclei which are sensitive to correlations arising from the short range part of the nucleon-nucleon interaction. One would therefore like to map out the nucleon momentum distributions over a wide range of momentum and energy transfer, starting from the low energy side where experimental results exist for ${}^3\text{He}^{(3)}$ and ${}^4\text{He}^{(4)}$.

2.2. Separation of Response Functions via Perpendicular Kinematics

In the perpendicular kinematic condition, Q^2 and the center of mass energy e_{cm} of the final system are held constant, so that the factorized single nucleon cross section and distortion effects do not vary. The energy and momentum distributions of the separated response functions can then be used to extract various distortion, off-shell and relativistic effects, meson exchange currents (MEC) and final state interactions (FSI) which would greatly help in constraining the various nuclear structure models.

In this proposal, we wish to avail of the dynamical range and flexibility of the CEBAF accelerator and spectrometers to extend the kinematical domain of the (e,e'p) measurements. We wish to extend the range in both Q^2 and recoil momentum p_m , while maintaining the condition for quasi-elastic scattering, $x = Q^2/2M\omega \approx 1$. To complete the program, one would like to extend the present proposal to include non-quasifree kinematics ($x \neq 1$), out-of-plane measurements and measurements of spin response functions.

By using simple invariance arguments, the unpolarized (e,e'p) cross sections can be written in a general, model independent form in terms of a set of response functions. For unpolarized electrons on an unpolarized target there are four response functions, σ_T , σ_L , σ_{LT} , σ_{TT} , and the cross section in terms of these partial cross sections is given by:

$$(5)$$

$$\frac{d^6\sigma}{de'dp'} = \Gamma_v \Sigma \quad (1)$$

where

$$\Sigma = \sigma_T + \epsilon(\sigma_L + \sigma_{TT} \cos 2\alpha) + \epsilon' \sigma_{LT} \cos \alpha$$

$$\Gamma_v = \frac{\alpha}{2\pi^2} \frac{e^2}{e_1} \frac{q}{Q^2} \frac{1}{1-\epsilon} \quad \text{is the virtual photon flux.}$$

Several kinematic domains are required to separate all the response functions and these are elaborated in references 5 and 6. Both Q^2 and the relative energy of the nucleon and the residual nucleus can be held fixed while varying p_m . One starts with $q = p'$ at $p_m = 0$, but then keeps e_{cm} and Q^2 constant as one increases p_m . A map of the response functions as a function of p_m can be obtained, by just varying γ_p (the angle between p' and q) keeping all other electron and hadron observables constant - much akin to measuring an angular distribution of the outgoing proton as a function of γ_p . In this condition, $x = Q^2/2M\omega$ is a constant, just slightly less than unity (due to the binding energy of the nucleus), and ensures that one stays on top of the quasielastic peak.

We wish to obtain separated response functions at Q^2 values ranging from 0.55 and 1.5 (GeV/c)² and missing momentum values upto 800 MeV/c. Two sets of kinematics are chosen, one at $q = 800$ MeV/c and the other at $q = 1.5$ GeV/c. These are schematically illustrated in figures 1 and 2. To separate the various response functions, three kinematical set-ups are required ($\Sigma_1, \Sigma_2, \Sigma_3$) to obtain σ_T, σ_{LT} and $\sigma_L + \sigma_{TT}$. One needs to go to an out-of-plane set-up Σ_4 to separate σ_L from σ_{TT} .

Configuration	α	γ_p		Σ_i
<u>Coplanar</u>				
1. Small $\theta_e(\epsilon_1)$	180°	$-\theta_p$	0	$\Sigma_1 = \sigma_T + \epsilon_1(\sigma_L + \sigma_{TT}) - \epsilon'_1\sigma_{LT}$
2. Small $\theta_e(\epsilon_1)$	0°	$+\theta_p$	0	$\Sigma_2 = \sigma_T + \epsilon_1(\sigma_L + \sigma_{TT}) + \epsilon'_1\sigma_{LT}$
3. Large $\theta_e(\epsilon_2)$	180°	$-\theta_p$	0	$\Sigma_3 = \sigma_T + \epsilon_2(\sigma_L + \sigma_{TT}) - \epsilon'_2\sigma_{LT}$
<u>Out of plane</u>				
4. Small $\theta_e(\epsilon_1)$	90°	0	$+\phi_p$	$\Sigma_4 = \sigma_T + \epsilon_1(\sigma_L - \sigma_{TT})$

$$\begin{aligned}\sigma_{LT} &= \left(\frac{1}{2\epsilon'_1}\right) [\Sigma_2 - \Sigma_1] \\ \sigma_T &= \left(\frac{1}{2\epsilon'_1(\epsilon_2 - \epsilon_1)}\right) [\Sigma_1(\epsilon'_1\epsilon_2 + \epsilon_1\epsilon'_2 + \Sigma_2(\epsilon'_1\epsilon_2 - \epsilon_1\epsilon'_2) - 2\epsilon'_1\epsilon_1\Sigma_3)] \\ \sigma_L + \sigma_{TT} &= \left(\frac{1}{2\epsilon'_1(\epsilon_2 - \epsilon_1)}\right) [-\Sigma_1(\epsilon'_1 + \epsilon'_2) + \Sigma_2(\epsilon'_2 - \epsilon'_1) + 2\epsilon_1\Sigma_3] \\ \sigma_{TT} &= \left(\frac{1}{4\epsilon_1}\right) [\Sigma_1 + \Sigma_2 - 2\Sigma_4]\end{aligned}$$

The (e,e'p) cross sections and count rates have been calculated with the code HE3EEX⁽⁷⁾ and also checked with the code MCEEP⁽⁸⁾. A luminosity of $10^{38}\text{cm}^{-2}\text{sec}^{-1}$ was assumed for all the runs, even though as shall be shown later, one can easily lower this significantly for the lower p_m runs without any loss in the determination of the errors of the response functions. The results of both the codes agree to a large extent, and for the purposes of this proposal, we used HE3EEX as it was less time consuming. The overlap of the acceptances in p_m for the three in-plane configurations are quite good and these are shown in figure 3 for $p_m = 300$ MeV/c. The codes assume the factorization of the cross section in PWIA into an elementary ep off-shell cross section and a single nucleon spectral function which contains the nuclear structure information:

$$\sigma_{eep} = \frac{1}{R} K \sigma_{ep} S(p_m, E_m) \quad (2)$$

where K is a kinematical factor and R is the recoil factor for scattering to a bound state of the residual nucleus. Here we have used the current conserved prescription "CC1" of deForest⁽⁹⁾ for σ_{ep} . For the single nucleon spectral function, we have used the calculations as given in reference 10. These calculations are by no means the most realistic or final, but just serve to evaluate the feasibility of performing this experiment under CEBAF conditions for the purposes of this proposal.

The $(e,e'p)$ cross sections in the four configurations ($\Sigma_1, \Sigma_2, \Sigma_3, \Sigma_4$) are shown in figure 4 for the $q = 800$ MeV/c and the $q = 1.5$ GeV/c cases. The corresponding separated response functions are shown in figure 5. The single arm quasielastic (e,e') cross sections were calculated with the code QFS⁽¹¹⁾ which employs a Fermi gas model to compute the quasielastic component and includes contributions from the delta and higher resonances. The single arm (e,p) cross sections have been calculated with the code EPC⁽¹¹⁾, which takes into account quasifree scattering, quasifree Δ production and two nucleon emission through quasideuteron model. The singles counting rates over the spectrometer acceptances are shown in figure 6 for both the electron and the proton arm. The coincident true and accidental counting rates for the three in-plane configurations are shown in figure 7.

Optimization of Counting Time

We have used the program EPERP⁽¹²⁾ to optimize the errors obtained for σ_T , σ_{LT} and $\sigma_L + \sigma_{TT}$ within the three in-plane configurations. The results are tabulated in Table 2 and shown in figure 8 for $q = 800$ MeV/c and in figure 9 for $q = 1.5$ GeV/c. As is very clear from this optimization study, the limiting factor in most of the p_m points is the systematic error of 2% rather than the statistics determined for each point. In fact, if one is able to improve the systematic error to 1%, the errors in the response functions are essentially halved, as is shown by the dashed curves in figure 8. *In most of these studies one invariably finds that the control of the systematic errors is the most important factor in the determination of the various response functions. The need for obtaining high statistics or luminosities has minimal effect, except in the cases of high recoil momenta where the cross sections are low.* We believe that a systematic error of 1.5% to 2% should

be achievable and depends critically on the determination of the incident electron energy, final electron momentum and in-plane angular determinations. The time required to obtain the statistics is minimal especially for the low p_m points and only becomes important at the highest values of p_m . This is especially true for the $q = 1.5$ GeV/c run. From figure 9, we find that for the $q = 1.5$ GeV/c run, we might only be able to effectively measure the σ_{LT} term, the error in the other two response functions increases dramatically after the $p_m = 400$ MeV/c point.

For the present proposal, we ask for a total of 340 hours for the $q = 800$ MeV/c run for ^3He . Similar times will be required for ^4He . The breakup of this time is shown in Table 1. No specific time is asked for the $q = 1.5$ GeV/c run for the present, and would be a natural extension once the $q = 800$ MeV/c run is completed.

Table 1 $q=800 \text{ MeV}/c$			
p_m	Σ	Time (hrs)	Statistical Errors
0	Σ_1	< 0.1	0.1%
	Σ_2	< 0.1	0.1%
	Σ_3	0.2	0.1%
100 MeV/c	Σ_1	0.2	0.1%
	Σ_2	0.25	0.1%
	Σ_3	2.5	0.2%
200 MeV/c	Σ_1	5.7	0.1%
	Σ_2	12.9	0.1%
	Σ_3	28.9	0.2%
300 MeV/c	Σ_1	31.6	0.1%
	Σ_2	30.1	0.2%
	Σ_3	27.8	0.4%
400 MeV/c	Σ_1	25.2	0.5%
	Σ_2	54.0	2.9%
	Σ_3	20.8	2.2%
500 MeV/c	Σ_1	17.6	1.0%
	Σ_2	65.4	9.6%
	Σ_3	17.0	4.2%
Total		340	

TABLE 2

REACTION $3He(e, ep)$

Mt = 2.8084GeV

Em = 0.0055GeV

My = 1.8757GeV

Sys error = 2.00%

Stat error = 0.10%

F1 = 0.20

Time = 100.00 hrs

Q= 0.800	Q2= 0.550	P= 0.800	PM= 0.000	S1=0.3008E-03(0.1%)	EP1=0.9710, T = 0.01 hrs,	CtST/hr = 0.6836E+08,	CtSA/hr = 0.9074E+0
				S2=0.3008E-03(0.1%)	EP2=0.9710, T = 0.01 hrs,	CtST/hr = 0.6836E+08,	CtSA/hr = 0.9074E+0
				S3=0.5580E-05(0.1%)	EP3=0.3080, T = 0.20 hrs,	CtST/hr = 0.4886E+07,	CtSA/hr = 0.2098E+0
				SigmaT = 0.1006E-01	DST(%) = 4.2		
				SigmaLTT=0.8159E-02	DSLTT(%) = 6.1		

Q= 0.800	Q2= 0.550	P= 0.796	PM= 0.100	S1=0.2626E-04(0.1%)	EP1=0.9710, T = 0.17 hrs,	CtST/hr = 0.5920E+07,	CtSA/hr = 0.1119E+0
				S2=0.1779E-04(0.1%)	EP2=0.9710, T = 0.25 hrs,	CtST/hr = 0.4010E+07,	CtSA/hr = 0.1696E+0
				S3=0.4594E-06(0.1%)	EP3=0.3080, T = 2.49 hrs,	CtST/hr = 0.4023E+06,	CtSA/hr = 0.1120E+0
				SigmaT = 0.7340E-03	DST(%) = 4.8		
				SigmaLTT=0.5999E-03	DSLTT(%) = 7.0		

Q= 0.800	Q2= 0.550	P= 0.783	PM= 0.200	S1=0.7951E-06(0.1%)	EP1=0.9710, T = 5.72 hrs,	CtST/hr = 0.1748E+06,	CtSA/hr = 0.6358E+0
				S2=0.3719E-06(0.1%)	EP2=0.9710, T = 12.89 hrs,	CtST/hr = 0.8178E+05,	CtSA/hr = 0.2228E+0
				S3=0.1333E-07(0.2%)	EP3=0.3080, T = 28.57 hrs,	CtST/hr = 0.1167E+05,	CtSA/hr = 0.8733E+0
				SigmaT = 0.1928E-04	DST(%) = 5.4		
				SigmaLTT=0.1607E-04	DSLTT(%) = 7.7		

Q= 0.800	Q2= 0.550	P= 0.763	PM= 0.300	S1=0.1507E-06(0.1%)	EP1=0.9710, T = 31.63 hrs,	CtST/hr = 0.3174E+05,	CtSA/hr = 0.6020E+0
				S2=0.5047E-07(0.2%)	EP2=0.9710, T = 30.12 hrs,	CtST/hr = 0.1063E+05,	CtSA/hr = 0.2836E+0
				S3=0.2452E-08(0.4%)	EP3=0.3080, T = 27.76 hrs,	CtST/hr = 0.2147E+04,	CtSA/hr = 0.8354E+0
				SigmaT = 0.3284E-05	DST(%) = 5.9		
				SigmaLTT=0.2810E-05	DSLTT(%) = 8.3		

Q= 0.800	Q2= 0.550	P= 0.733	PM= 0.400	S1=0.8308E-08(0.5%)	EP1=0.9710, T = 25.20 hrs,	CtST/hr = 0.1643E+04,	CtSA/hr = 0.3268E+0
				S2=0.2098E-08(2.9%)	EP2=0.9710, T = 53.97 hrs,	CtST/hr = 0.4148E+03,	CtSA/hr = 0.3708E+0
				S3=0.1324E-09(2.2%)	EP3=0.3080, T = 20.83 hrs,	CtST/hr = 0.1159E+03,	CtSA/hr = 0.8571E+0
				SigmaT = 0.1676E-06	DST(%) = 8.5		
				SigmaLTT=0.1476E-06	DSLTT(%) = 10.0		

Q= 0.800	Q2= 0.550	P= 0.695	PM= 0.500	S1=0.3364E-08(1.0%)	EP1=0.9710, T = 17.60 hrs,	CtST/hr = 0.6090E+03,	CtSA/hr = 0.2624E+0
				S2=0.6804E-09(9.6%)	EP2=0.9710, T = 65.44 hrs,	CtST/hr = 0.1232E+03,	CtSA/hr = 0.4514E+0
				S3=0.5280E-10(4.2%)	EP3=0.3080, T = 16.96 hrs,	CtST/hr = 0.4624E+02,	CtSA/hr = 0.9407E+0
				SigmaT = 0.6416E-07	DST(%) = 13.3		
				SigmaLTT=0.5841E-07	DSLTT(%) = 13.5		

${}^3\text{He}(e,e'p)d$

$M_T = 2.808 \text{ GeV}$
 $E_m = 5.49 \text{ MeV}$

Perpendicular

$E_{cm} = 190 \text{ MeV}$
 $W = 3.004 \text{ GeV}$

$q = 0.800 \text{ GeV}/c$
 $Q^2 = 0.550 \text{ (GeV}/c)^2$
 $w = 300 \text{ MeV}$

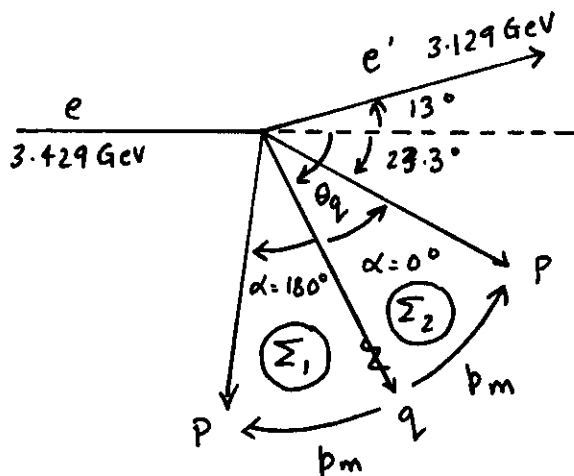
Kinematics:

$p_m = 0$ $p' = q = 0.800 \text{ GeV}/c; T_P = 295 \text{ MeV}$
 $p_m = 500 \text{ MeV}/c$ $p' = 0.695 \text{ GeV}/c; T_P = 229 \text{ MeV}$

$\lambda = Q^2/q^2 = 0.859$
 $x = Q^2/2m_p w = 0.976$

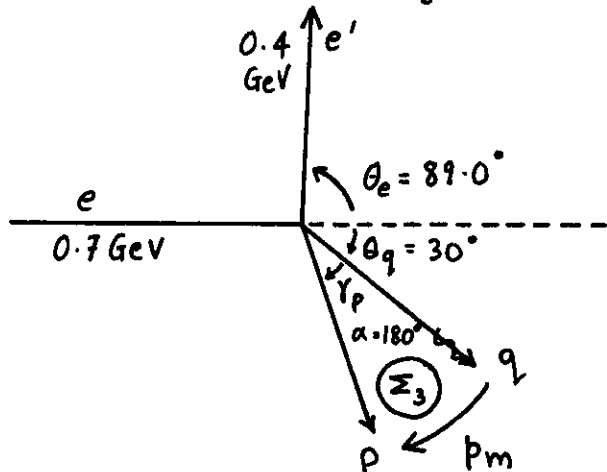
Forward Kinematics Σ_1, Σ_2

$\epsilon_1 = 0.971$
 $\epsilon_1' = 1.381$
 $\sigma_M = 2.65 \mu\text{b}$



p_m MeV/c	γ_P°	Σ_1	Σ_2	Σ_3
0	0	61.6	61.6	30.0
100	7.2	68.8	54.4	37.2
200	14.5	76.1	47.1	44.5
300	22.0	83.6	39.6	52.0
400	29.8	91.5	31.8	59.8
500	38.3	99.9	23.3	68.3

Backward Kinematics Σ_3



$\epsilon_2 = 0.308$
 $\epsilon_2' = 0.635$
 $\sigma_M = 0.0223 \mu\text{b}$

Figure 1

$^3\text{He}(e,e'p)d$

$M_T = 2.808 \text{ GeV}$

$E_m = 5.49 \text{ MeV}$

Perpendicular

$E_{cm} = 508 \text{ MeV}$

$q = 1.500 \text{ GeV}/c$

Kinematics:

$W = 3.322 \text{ GeV}$

$Q^2 = 1.550 (\text{GeV}/c)^2$

$\omega = 836 \text{ MeV}$

$p_m = 0$ $p' = q = 1.50 \text{ GeV}/c; T_p = 831 \text{ MeV}$

$\lambda = Q^2/q^2 = 0.689$

$p_m = 800 \text{ MeV}/c$ $p' = 1.303 \text{ GeV}/c; T_p = 667 \text{ MeV}$

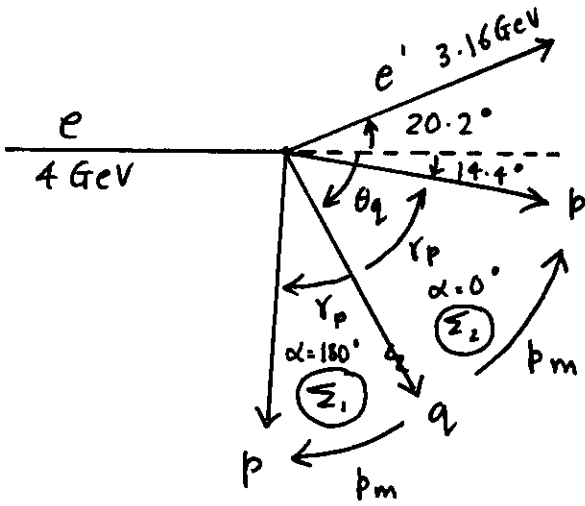
$x = Q^2/2m_p\omega = 0.988$

Forward Kinematics Σ_1, Σ_2

$\epsilon_1 = 0.916$

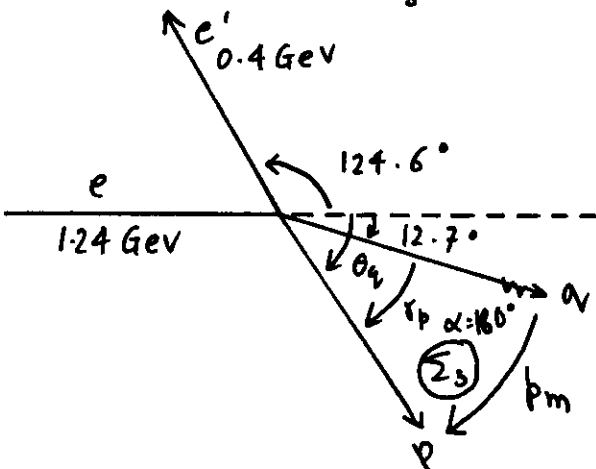
$\epsilon_1' = 1.325$

$\sigma_M = 0.335 \mu\text{b}$



p_m MeV/c	γ_p°	Σ_1	Σ_2	Σ_3
0	0	46.6	46.6	12.7
200	7.7	54.3	39.0	20.3
400	15.5	62.1	31.2	28.2
600	23.6	70.2	23.0	36.3
800	32.2	78.8	14.4	44.9

Backward Kinematics Σ_3



$\epsilon_2 = 0.087$

$\epsilon_2' = 0.308$

$\sigma_M = 0.0119 \mu\text{b}$

Figure 2

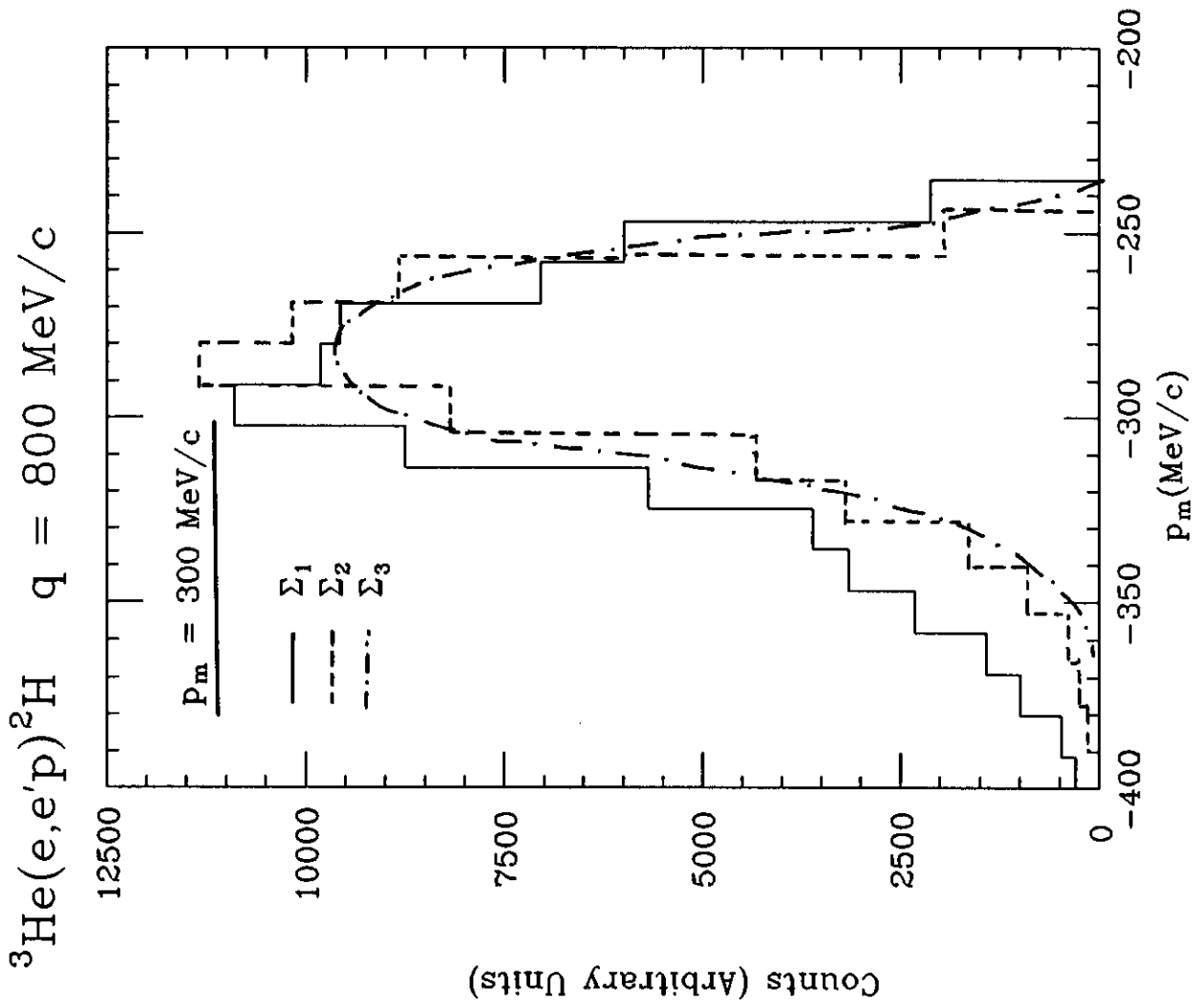
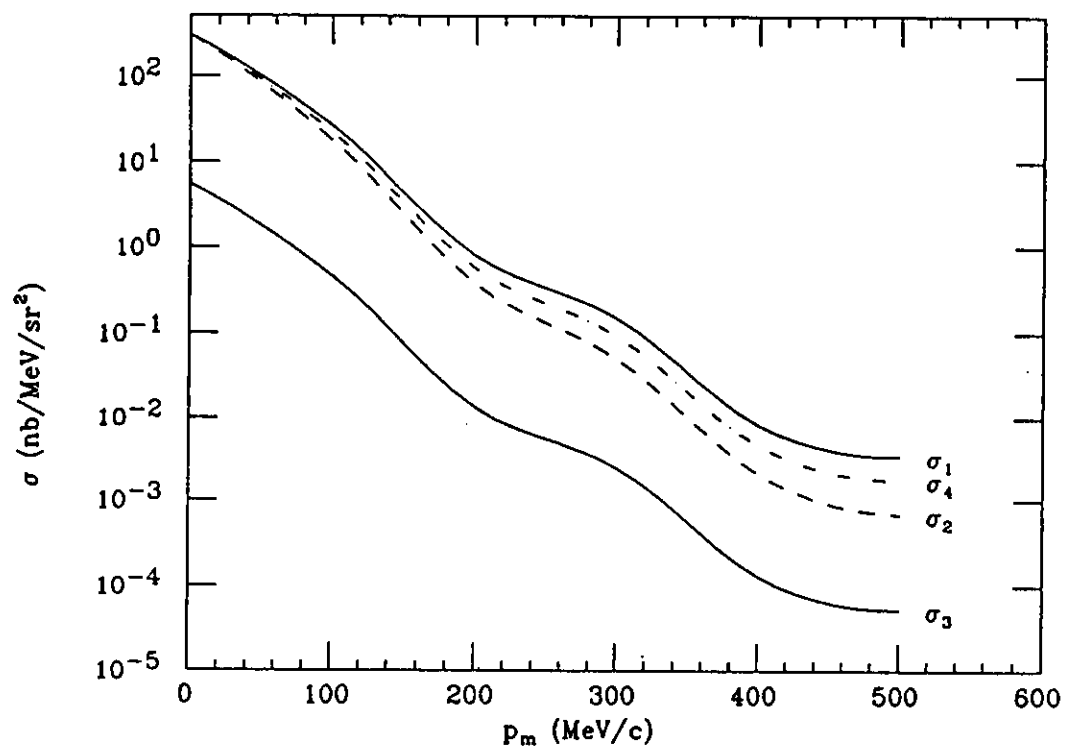


Figure 3

${}^3\text{He}(e,e'p){}^2\text{H}$ $q = 800 \text{ MeV}/c$



${}^3\text{He}(e,e'p){}^2\text{H}$ $q = 1500 \text{ MeV}/c$

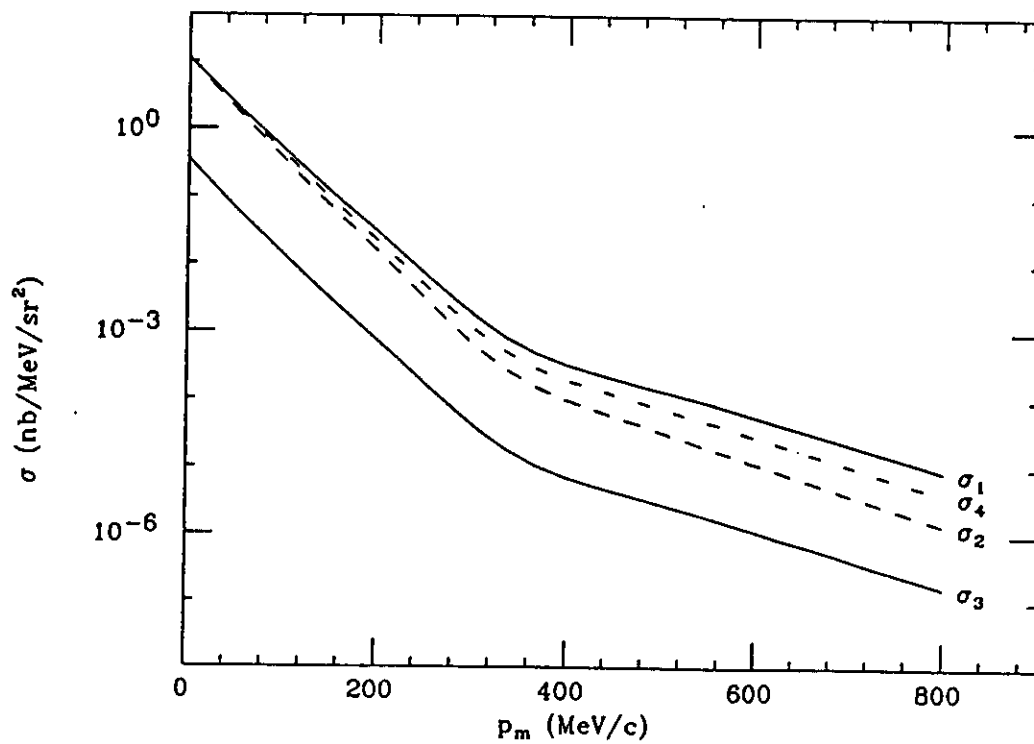
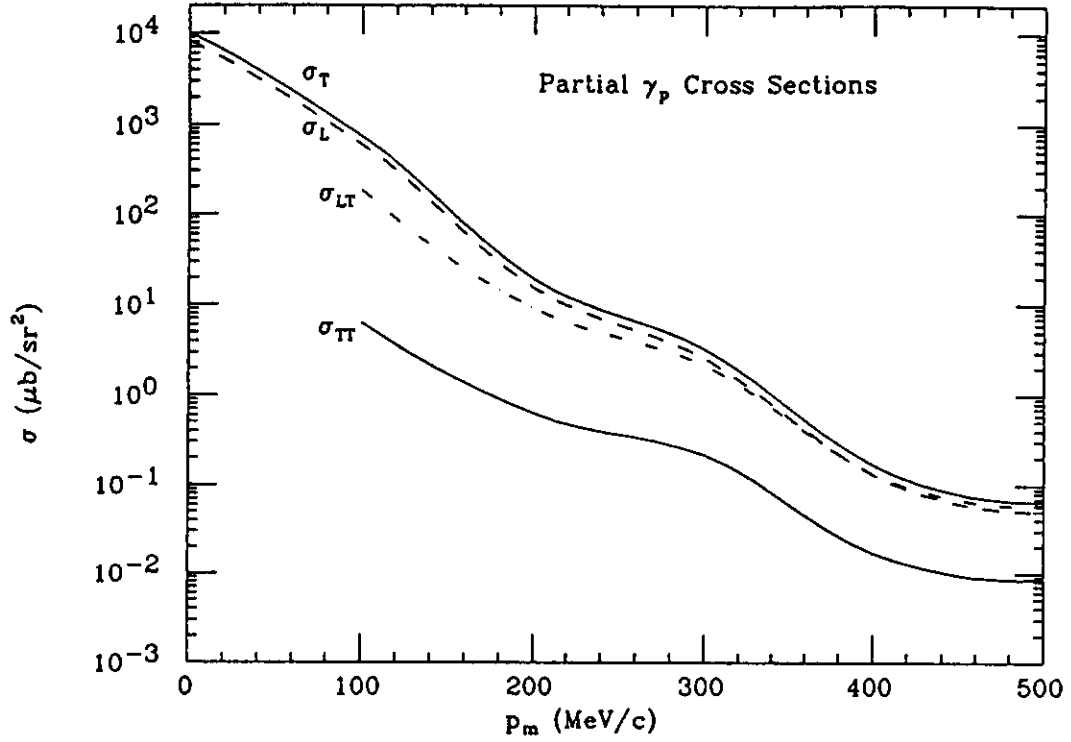


Figure 4

${}^3\text{He}(e,e'p){}^2\text{H}$ $q = 800 \text{ MeV}/c$



${}^3\text{He}(e,e'p){}^2\text{H}$ $q = 1500 \text{ MeV}/c$

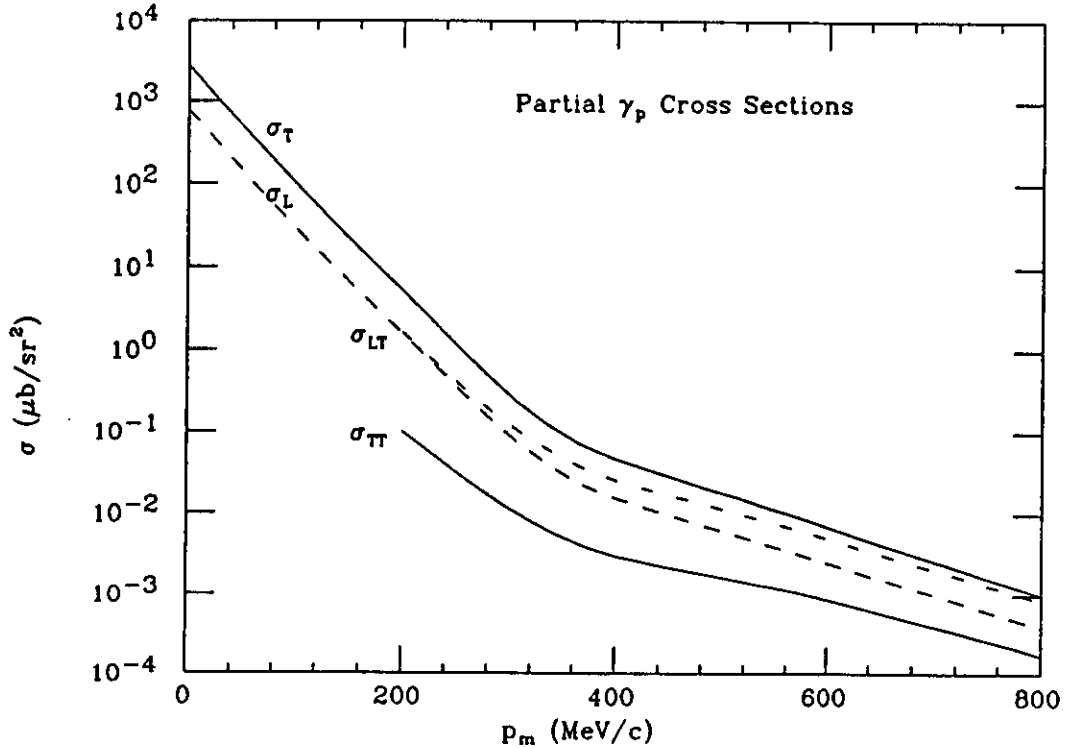


Figure 5

${}^3\text{He}(e,e'p){}^2\text{H} \quad q = 800 \text{ MeV}/c$

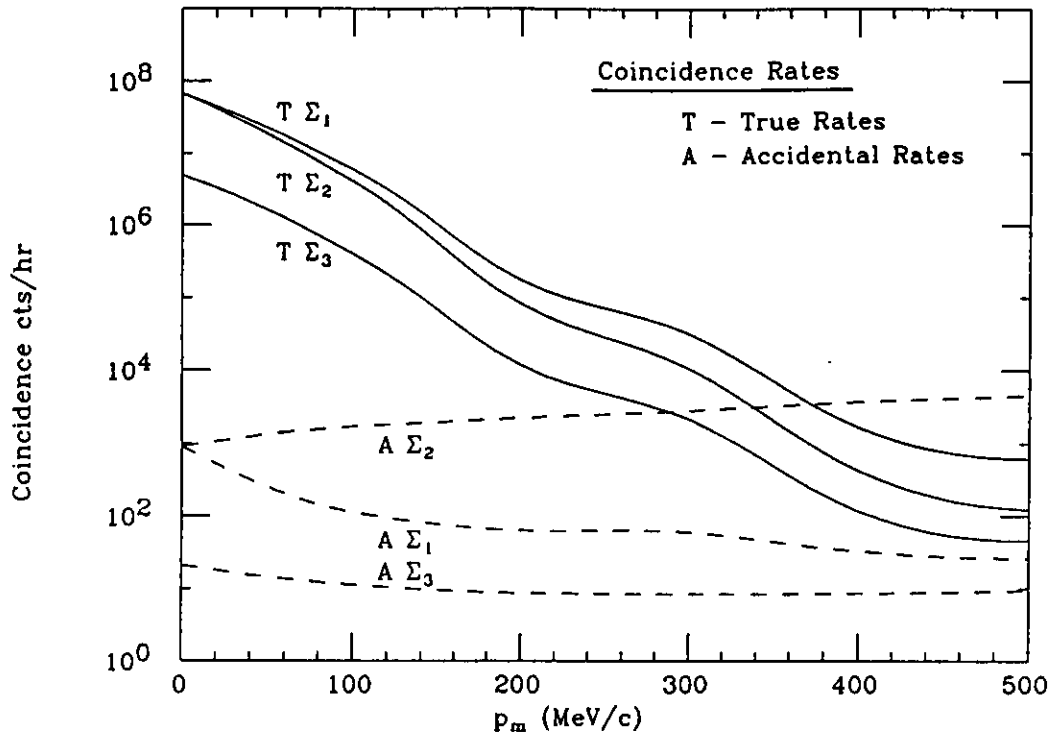


Figure 7

${}^3\text{He}(e,e'p){}^2\text{H} \quad q = 800 \text{ MeV}/c$

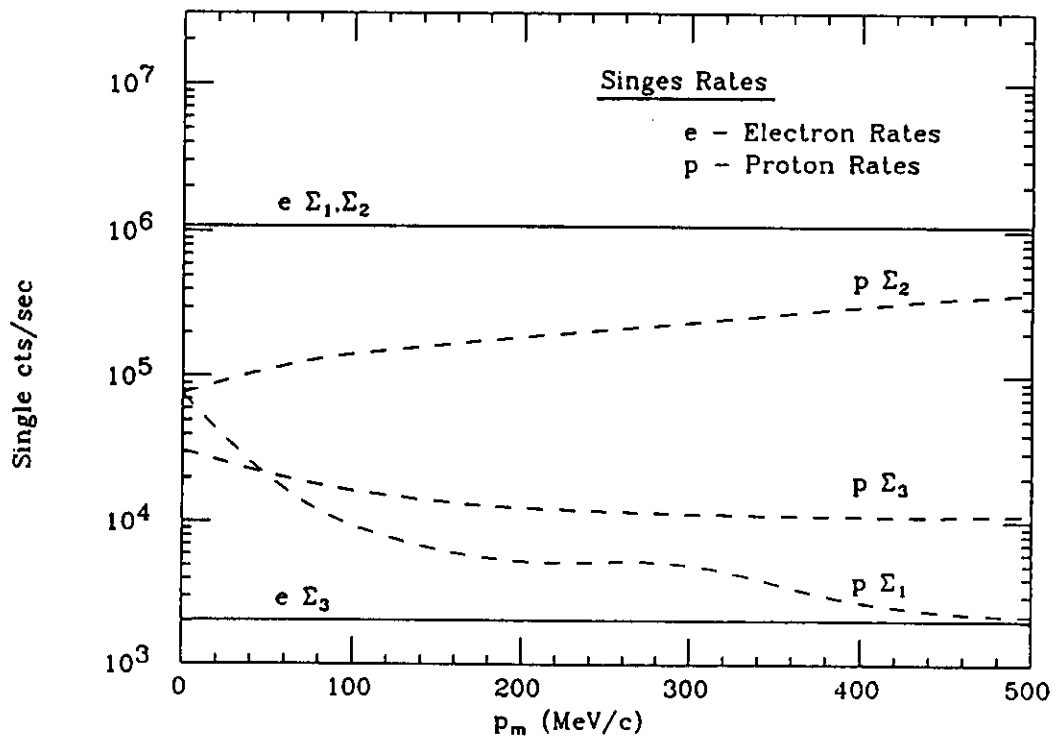


Figure 6

${}^3\text{He}(e,e'p){}^2\text{H}$ $q = 800 \text{ MeV}/c$

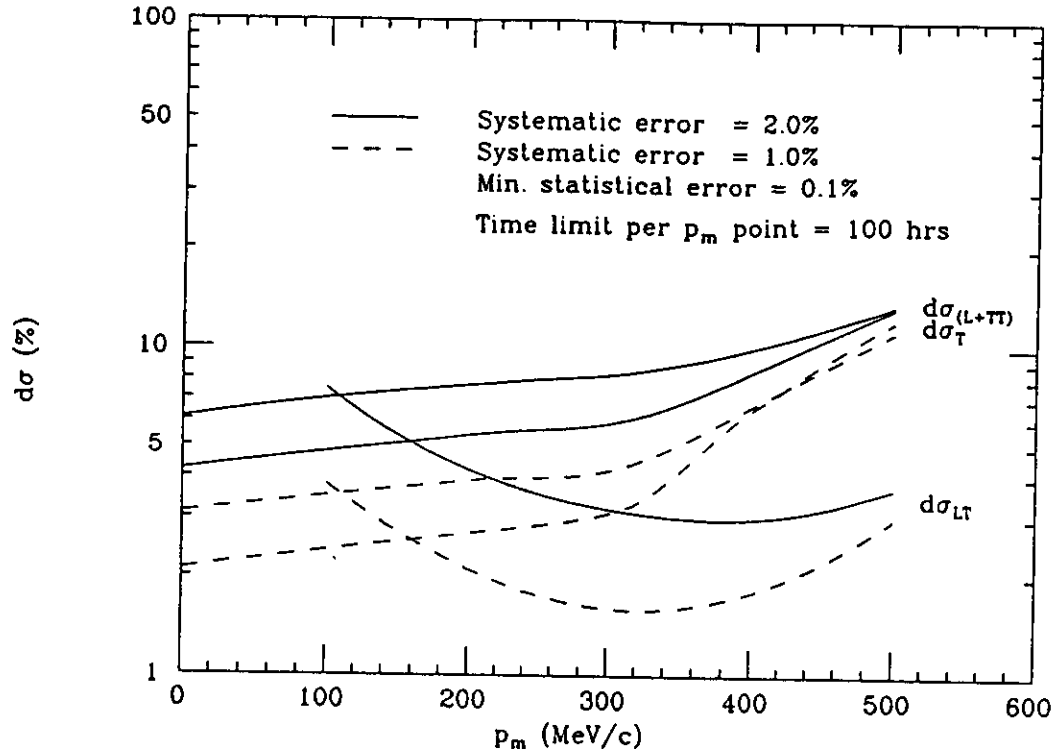
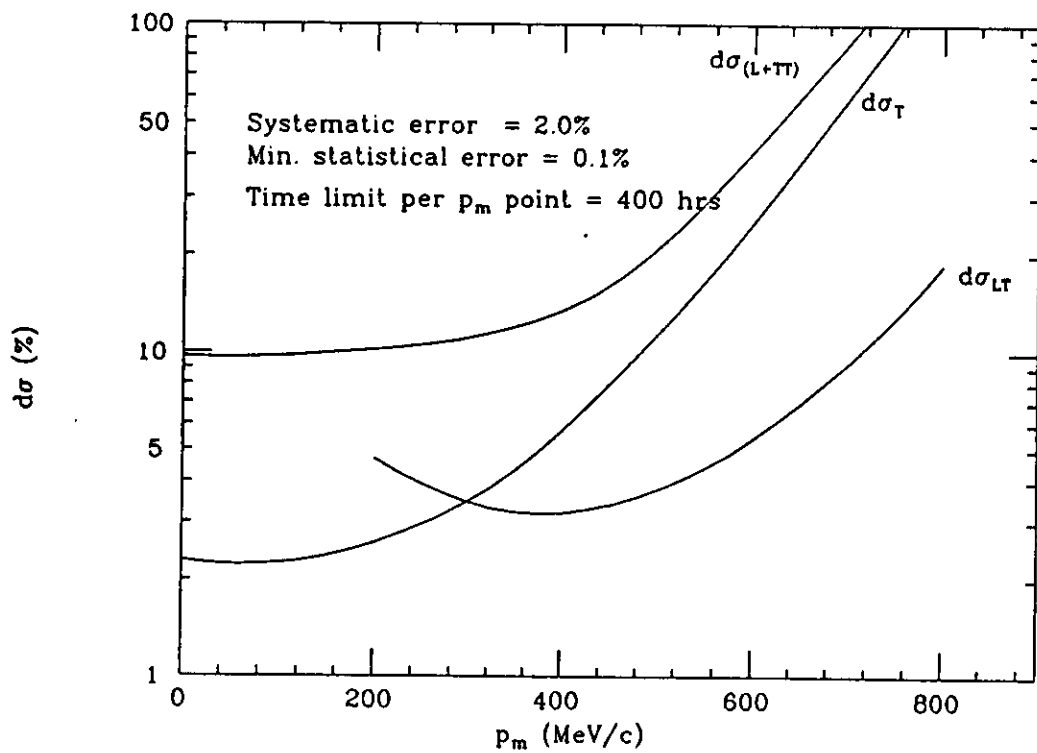


Figure 8

${}^3\text{He}(e,e'p){}^2\text{H}$ $q = 1500 \text{ MeV}/c$



Part 2 : The Q^2 Dependence of the Longitudinal and Transverse Response Functions

2.1. Physics motivation

In the standard approach of electron scattering, it is assumed that the nuclear current is a superposition of individual nucleon currents essentially identical to the free nucleon ones (impulse approximation, IA). Under this approximation, the electromagnetic responses give direct access to single nucleon densities^[13]. Indeed, such description has been found to be adequate to describe the first systematic quasielastic inclusive data^[14] as well as coincidence (e,e'p) results at modest values of Q^2 . However, the experimental separation of the longitudinal and transverse response function for *inclusive quasielastic scattering*, over a wide range of nuclei has produced evidence for a breakdown of this simple model. The *transverse* response is found to *agree reasonably well* with traditional nuclear theory calculations, once two-body effects from meson-exchange and short range correlations are taken into account. However, *strength is missing in the longitudinal part*, as indicated for example in longitudinal sum rule results.

Combined with the observations of the EMC effect^[15], the question of a possible modification of the nucleon structure in the nuclear medium has been raised. The single-nucleon current j_μ has basically three ingredients; the nucleon spinors, the nucleon electromagnetic form factors and the form of the current operator itself:

$$\begin{aligned} j_\mu &= \bar{u}(\vec{p}') \left[F_1(Q^2) \gamma_\mu + \frac{i\kappa}{2M} F_2(Q^2) \sigma_{\mu\nu} q^\nu \right] u(\vec{p}) \\ &= \bar{u}(\vec{p}') \left[(F_1(Q^2) + \kappa F_2(Q^2)) \gamma_\mu - \frac{\kappa}{2M} F_2(Q^2) (p'_\mu + p_\mu) \right] u(\vec{p}) \quad . \end{aligned} \quad (1)$$

The two forms of j_μ , related by the Gordon identity, are only equivalent *on-shell*.

Relativistic mean-field theories^[16] predict a nucleon-energy-dependent modification of the nucleon spinors while in other approaches the form factors themselves may depend on nuclear density^[17], resulting in a different Q^2 dependence than for free nucleons.

Experimentally, the situation is somehow controversial. For single arm experiments, the longitudinal responses are found significantly reduced relative to

theoretical expectations, except however for ${}^2\text{H}$ [18], ${}^3\text{H}$, [19], ${}^3\text{He}$ [19],[20] and possibly ${}^4\text{He}$ [18]. For the heavier systems, the approaches mentioned above give some agreement with data for the longitudinal response (see figure 1), but none of them can reproduce in a consistent way the existing set of experimental results.

Coincidence experiments including longitudinal/transverse separations have been performed in the last few years at NIKHEF [21],[4], Saclay [22],[23] and Bates [24], however in a very limited range of momentum transfer values. Although the coincidence data show also a lack of longitudinal strength in accordance with the single arm results, the momentum transfer dependence of the transverse response for the ${}^{40}\text{Ca}(e,e'p)$ reaction does not depart (at the few % level) from what is expected from free nucleon currents [22]. A longitudinal/transverse separation for the ${}^4\text{He}(e,e'p){}^3\text{H}$ reaction has been performed recently up to $q=0.7\text{GeV}/c$ (see figure 3) by Magnon et al. [23]. After final state interaction (FSI) and meson exchange current (MEC) corrections are applied, the q -dependence of the data are consistent with the impulse approximation, but the longitudinal/transverse ratio is 30 predicted. Although the data may indicate a trend for a larger deviation at higher q , the statistical accuracy is insufficient to conclude.

All of the coincidence results discussed above correspond to low values of the missing (or internal) momentum and separation (binding) energy. One knows that, in principle, more than two form factors are necessary to describe off-mass-shell nucleons [25]. The CEBAF high energy continuous beam will be a unique tool to extend the studies mentioned above to more strongly bound nucleons, over a large range of high Q^2 values.

We intend to explore the longitudinal and transverse response functions in the He isotopes to the highest practical Q^2 . We will make our measurements in parallel kinematics (\vec{p}'/\vec{q}) so as to eliminate the contributions from the interference response functions σ_{TL} and σ_{TL} . The $(e,e'p)$ cross section then contains only two response functions, when the beam and target are unpolarized and no final state polarizations are observed. These are the longitudinal (σ_L) and the transverse (σ_T):

$$\frac{d^5\sigma}{de'd\Omega_e d\Omega_p} = \Gamma_v [\sigma_T + \epsilon\sigma_L] \quad , \quad (2)$$

where Γ_ν is the virtual photon flux

$$\Gamma_\nu = \frac{\alpha}{2\pi^2} \frac{e'}{e} \frac{q}{Q^2} \frac{1}{(1-\epsilon)} \quad , \quad (3)$$

and ϵ is the longitudinal virtual photon polarization defined as

$$\epsilon = \left[1 + \frac{2\bar{q}^2}{q_\mu^2} \tan^2(\theta/2) \right]^{-1} . \quad (4)$$

The response functions can be separated by measurements in the (e, e') plane by the standard Rosenbluth technique. In PWIA, the coincidence cross section may be written as:

$$\frac{d^5\sigma}{de'd\Omega_e d\Omega_p} = K \sigma_{ep} S(\vec{p}, E_m) \quad , \quad (5)$$

where σ_{ep} is the cross section for electron scattering from a proton of momentum \vec{k} (which contains the two *nucleon* structure functions) and $S(\vec{p}, E_m)$, the nuclear spectral function, is the joint probability of finding a proton of momentum $\vec{p} = \vec{p}' - \vec{q} = -\vec{p}_m$ within the nucleus and leaving the residual system with an excitation energy E_m . We will keep these quantities, thus the spectral function fixed so as to obtain information on σ_{ep} . Of course, the final state interactions destroy this simple factorization approximation so we will use the best available unfactorized calculations to analyze the data.

3.2. Proposed measurements

We propose to measure the cross section for the ${}^3\text{He}(e, e')p$ d and ${}^4\text{He}(e, e')p$ ${}^3\text{H}$ reactions in parallel kinematics, at several momentum transfer values. For each of them, measurements will be done at two different beam energies and corresponding electron angles to separate the longitudinal and transverse parts of the cross section. As we show later, the high resolution of the Hall A spectrometers is needed, not only to clearly identified the two-body break-up process and optimize the true/accidental coincidence ratio, but also to control the systematic uncertainties in the separations.

The kinematics are given in Table 1 in the case of ${}^3\text{He}$. Points 1F to 4B are centered at missing (recoil) momentum, $p_m = 0$. The lowest momentum transfer value, $q=0.6$ GeV/c, allow an overlap with existing (or planned in the near future)

measurements. In addition, we have included kinematics with non-zero missing momentum (points 5F to 8B) to study the Q^2 dependence of the response functions for off-shell nucleons. The selected value, $p_m = 0.3 \text{ GeV}/c$, should be large enough to exhibit a possible p_m effect, still allowing sufficient cross-section. Both parallel and antiparallel configuration are considered for each Q^2 value. One can see that, as the $p_m=0$. points are at the top of the quasielastic peak, $p_m > 0$. and $p_m < 0$. are on the low and high energy side respectively. In arriving at these kinematics, minimum momenta of $0.4 \text{ GeV}/c$ and minimum angles of 12.5° were considered for both spectrometers. In addition, a maximum beam energy of 4 GeV was assumed. A larger beam energy would be advantageous for the higher \vec{q} points since it would allow more forward electron angles giving higher counting rates and better virtual photon polarization lever arms.

3.3. Cross sections and acceptances calculations

Although it is our intend to perform the measurements on both ^3He and ^4He , the cross sections and counting rates have been estimated in some detail for the ^3He case only.

The $(e,e'p)$ cross sections were calculated using the computer program CARLEEP, an updated version of CARLOUT [26]. This program performs an averaging of the cross section and its various components over the experimental acceptances and allow the evaluation of realistic count rate estimates for any desired kinematical cut. Some of us paid particular attention to these finite acceptance effects in the past [27], as they can strongly affect the count rates and the accuracy of the final result. For the case of interest here, the quite large momentum and angular acceptances of the Hall A spectrometers define complex and correlated acceptances in the *physical* variables (Q^2 , E_m , \vec{p}_m , and γ_{cm}) on which the response functions σ_T and σ_L depend. As shown in figure 3, these acceptances differ strongly in forward and backward kinematics. One then has first to make cuts to define overlapping regions for averaging the cross sections and structure functions. However, within these cuts, the probability distribution of a given variable is quite different in the two kinematics. To make sure that the separation method is meaningful, one must ensure that the average values of the physical variables and structure

functions to be extracted remain the same to some level of accuracy. Then a model can be used, for example the one built in CARLEEP itself, or a more sophisticated one, to compute the correcting factors f_{TF} , f_{LF} , f_{TB} and f_{LB} needed to relate the experimental averaged cross sections to the structure functions σ_T and σ_L in a well defined (e.g. center of acceptances) kinematics. These are the quantities to be extracted and compared to theory. The f_{ij} 's are defined as :

$$\sigma_F^{exp.} = f_{TF}\sigma_T + \epsilon_F f_{LF}\sigma_L \quad , \quad (6)$$

$$\sigma_B^{exp.} = f_{TB}\sigma_T + \epsilon_F f_{LB}\sigma_L \quad . \quad (7)$$

The following cuts have been considered (see Table 2):

- a) Only events associated with 2-body break-up have been generated.
- b) For each Q^2 , the backward angle acceptance is used to define cuts in Q^2 .
- c) For each of the three p_m values (0., ± 0.3 GeV/c), the backward angle acceptance is used to define cuts in p_m .
- d) No cuts have been put on angles.

The effect of these cuts is shown in Table 3 on an example. One notices also that there is a non-zero contribution (listed under σ_{rea}) of the TT and TL interference terms, which do not contribute when \vec{q} and \vec{p}' are strictly colinear.

The coincidence cross sections are listed in Table 4. As mentioned in the introduction, the single electron and proton rates have been calculated using the computer codes QFSV and EPC respectively. The EPC code was also used to compute (e,π^+) and (e,π^-) cross sections. These cross sections, integrated over the momentum acceptance of the spectrometers are also listed in Table 4. Correlated backgrounds from $(e,e'\pi^+)$ and (γ,π^-p) have been neglected. The $(e,e'\pi^+)$ process is not allowed kinematically for these experiments. Moreover, at the quasielastic kinematics, the (γ,π^-p) process requires a photon energy near the endpoint. Thus, we do not expect this process to dominate the correlated yield. However, especially for the $p_m = -0.3$ GeV/c case, it would be desirable to have actual estimates of the contribution of these processes.

3.3. Counting rates and beam time request

The counting rates have been calculated assuming a luminosity of $= 1. \times 10^{38}$ $\text{cm}^{-2}\text{sec}^{-1}$. A coincidence resolving time of 4 ns (full width at base) is assumed for the accidentals rates. These are given in a 5 MeV missing energy bin. Both time and energy resolution can possibly be improved. One sees that accidentals are totally negligible for the $p_m = 0$. points. The use of both shower and Čerenkov detectors will allow a e/π rejection ratio of $\sim 10^5$ which is sufficient in view of the cross section values (Table 4). One assumes also that the detectors will be adequately shielded. As a result, the accidental rates have been determined considering only the true single electron and proton rates. The counting rates are listed in Table 5.

The counting times for each (forward/backward) combination have been optimized for a fixed luminosity value of $= 1. \times 10^{38}$ $\text{cm}^{-2}\text{sec}^{-1}$ and assuming an overall 1% systematic uncertainty for all cross section determinations. The optimization criterium is an error on the determination of σ_L not worse than twice the corresponding one for an infinitely good statistics. Again, one sees from Table 6 that the counting time requested for the $p_m = 0$. measurements is fairly small, and that the luminosity can be easily reduced by a factor of 2 to 5 if the data rates are a problem. Most of the time will be spent on the $p_m = \pm 0.3$ GeV/c points at backward angle.

Using the computer code SIGEEP^[28] a sensitivity analysis was performed to estimate the uncertainty in the (e,e'p) cross section due to uncertainties in the momenta and angles of the detected particles. The total error is computed assuming the following measurement uncertainties :

$$\begin{array}{ll} \delta e/e & \pm 1 \times 10^{-4} \\ \delta e'/e' & \pm 1 \times 10^{-4} \\ \delta \theta_b/\theta_b & \pm 0.1 \text{ mr} \\ \delta \theta/\theta & \pm 0.1 \text{ mr} \end{array}$$

$$\delta\theta_p/\theta_p$$

$$\pm 0.1 \text{ mr}$$

The results are given in Table 7. The error estimates are computed assuming these quantities are known to this precision in an absolute sense. The method of determining absolute energies of both the beam and detected particles to these levels will have to be established in some detail for such estimates to apply.

Once schemes will be defined for operating the three CEBAF end stations simultaneously, the kinematics may have to be adjusted to minimize the number of energy changes and facilitate the beam sharing. Including an additional 35 hrs for energy/angle changes and some control measurements, 250 hrs are asked for these measurements.

Table 1
Kinematics for L/T Separations

Kin	P_m (GeV/c)	\bar{q} (GeV/c)	Q^2 (GeV/c) ²	ω (GeV)	T_p (GeV)	e (GeV)	e' (deg)	θ_e (deg)	θ_p (deg)	ϵ
1F	0	0.6	0.327	0.181	0.175	2.719	2.538	12.5	66.3	0.974
1B	0	0.6	0.327	0.181	0.175	0.581	0.400	72.8	39.6	0.456
2F	0	1.0	0.808	0.439	0.433	4.000	3.561	13.7	57.4	0.966
2B	0	1.0	0.808	0.439	0.433	0.839	0.400	101.8	23.1	0.211
3F	0	2.0	2.371	1.276	1.271	4.000	2.724	27.0	38.2	0.837
3B	0	2.0	2.371	1.276	1.271	1.753	0.477	114.7	12.5	0.108
4F	0	3.0	4.113	2.311	2.205	4.000	1.789	44.6	24.7	0.577
4B	0	3.0	4.113	2.311	2.205	2.863	0.653	95.8	12.5	0.157
5F	0.3	0.717	0.5	0.118	0.088	3.308	3.190	12.5	74.3	0.976
5B	0.3	0.717	0.5	0.118	0.088	0.518	0.400	102.0	33.1	0.242
6F	0.3	1.040	1.0	0.286	0.257	4.000	3.714	14.9	66.7	0.964
6B	0.3	1.040	1.0	0.286	0.257	0.686	0.400	145.2	12.8	0.043
7F	-0.3	0.979	0.5	0.677	0.648	3.603	2.925	12.5	40.3	0.956
7B	-0.3	0.979	0.5	0.677	0.648	1.077	0.400	65.1	21.8	0.390
8F	-0.3	1.507	1.0	1.127	1.098	4.000	2.873	17.0	33.8	0.908
8B	-0.3	1.507	1.0	1.127	1.098	1.527	0.400	79.6	15.1	0.241

Table 2
Q² and p_m cuts

Kinematics	p _m (GeV/c)	Q ² cuts (GeV/c) ²	p _m cuts (GeV/c)
2(F + B)	0.	0.76 – 0.86	0. – 0.075
3(F + B)	0.	2.25 – 2.48	0. – 0.075
4(F + B)	0.	3.90 – 4.25	0. – 0.075
5(F + B)	0.3	0.485 – 0.515	0.27 – 0.33
6(F + B)	0.3	0.900 – 1.100	0.27 – 0.33
7(F + B)	-0.3	0.480 – 0.530	0.28 – 0.32
8(F + B)	-0.3	0.950 – 1.050	0.28 – 0.32

Table 3
Finite acceptance effects in kinematics 2

	σ _T nb/sr	σ _L nb/sr	σ _{res} nb/sr	σ nb/sr	Q ² (GeV/c) ²	P _m (GeV/c)	γ _{cm} (deg)
Forward: F	46.4	25.5	-0.47	66.3	0.8100	0.0481	3.98
Backward: B	51.0	28.0	-1.73	55.2	0.8086	0.0439	3.55
$A = \frac{B+F}{2}$	48.7	26.8					
$\frac{B-F}{A}$	9.5%	9.5%					
From σ : S	52.1	14.7					
$\frac{S-A}{A}$	6.9%	-45.0%					

Table 4
Single and Coincidence cross-sections

Kinematics	(e,e')	(e, π^-)	(e,p)	(e, π^+)	(e,e'p)
	nb/br	nb/br	nb/br	nb/br	nb/sr ⁻² /Gev
1F	3155	13.9	270.6	65.8	
1B	21.5	0.63	0	0	
2F	314	17.9	104.4	94.5	60450.
2B	0.64	1.10	129.5	0	1173.
3F	1.455	17.3	1342	71.1	826.
3B	0.0111	2.09	1397	0.	55.
4F	0.0355	14.6	910	19.5	48.2
4B	0.0028	4.89	1016	0.	11.8
5F	718	1.37	406	85.3	28.5
5B	0.671	0	795	34.7	0.656
6F	35	0	46.6	91.4	8.27
6B	0.078	0	426.	0.	0.162
7F	717	36.5	2530.	97.5	40.1
7B	3.30	15.2	379.	0.	1.19
8F	83	37.5	2055.	106.4	4.94
8B	0.485	16.0	1348.	0.	0.186

Table 5
Counting Rates

Kin	$\Delta e'$ GeV	$\Delta T'$ GeV	N_e (sec ⁻¹)	N_p (sec ⁻¹)	f	trues (sec ⁻¹)	accid. (sec ⁻¹)	<u>trues</u> accid.
1F	0.254	0.049	2.5(+6)	2.1(+5)				
1B	0.040	0.049	1.7(+4)	1.7(+5)				
2F	0.356	0.109	2.4(+5)	1.1(+5)	0.070	1870.	0.10	
2B	0.040	0.109	500.	1.0(+5)	0.892	255.	8(-3)	
3F	0.272	0.272	1.1(+3)	1.0(+6)	0.095	86.7	8.(-3)	
3B	0.048	0.272	8.7	1.1(+6)	0.409	6.53	3(-4)	
4F	0.179	0.429	28.	7.1(+5)	0.112	5.89	1.(-4)	
4B	0.065	0.429	2.2	7.9(+5)	0.175	0.823	1.(-5)	
5F	0.319	0.025	5.6(+5)	3.2(+5)	0.100	0.293	0.	2.6
5B	0.040	0.025	520.	6.2(+5)	0.989	0.067	0.159	0.42
6F	0.371	0.069	2.7(+4)	3.6(+4)	0.225	0.518	0.012	44.
6B	0.040	0.069	61.	3.3(+5)	0.606	0.024	0.006	4.
7F	0.293	0.155	5.6(+5)	2.0(+6)	0.086	2.17	6.58	0.33
7B	0.040	0.155	2.6(+3)	3.0(+5)	0.741	0.214	0.075	2.9
8F	0.287	0.241	6.5(+4)	1.6(+6)	0.108	0.519	0.78	0.66
8B	0.040	0.241	380.	1.1(+6)	0.709	0.032	0.025	1.3

Table 6
Running Time and Errors

Kin	p_m GeV/c	Running F (hours)	Time B	$\delta\sigma_F/\sigma_F$ (%,stat)	$\delta\sigma_B/\sigma_B$ (%,stat)	$\delta\sigma_T/\sigma_T$ (%,tot)	$\delta\sigma_L/\sigma_L$ (%,tot)
1	0.	0.3	0.7				
2	0.	0.3	0.7	0.07	0.13	1.4	8.2
3	0.	0.2	0.8	0.37	0.74	1.5	18.3
4	0.	2	4	0.53	0.88	1.9	40.0
5	0.3	14	46	1.11	2.27	3.5	29.3
6	0.3	7	33	0.89	2.30	2.6	14.5
7	-0.3	8	12	1.04	1.37	3.3	20.9
8	-0.3	21	59	1.00	1.95	3.2	15.8

Total 209

Table 7
Kinematical Systematic Uncertainties in Cross Section

Kin	e %/MeV	θ_b %/mr	e' %/MeV	θ_e %/mr	θ_p %/mr	Total %
1F	0.022	2.32	0.14	2.33	0.001	0.33
1B	0.014	0.41	0.44	0.30	0.12	0.06
5F	17.0	26.8	18.8	26.9	0.19	9.06
5B	12.4	2.41	24.9	2.32	0.07	1.23
7F	1.61	6.47	2.16	6.19	0.32	1.24
7B	1.33	1.00	4.17	1.16	0.18	0.27

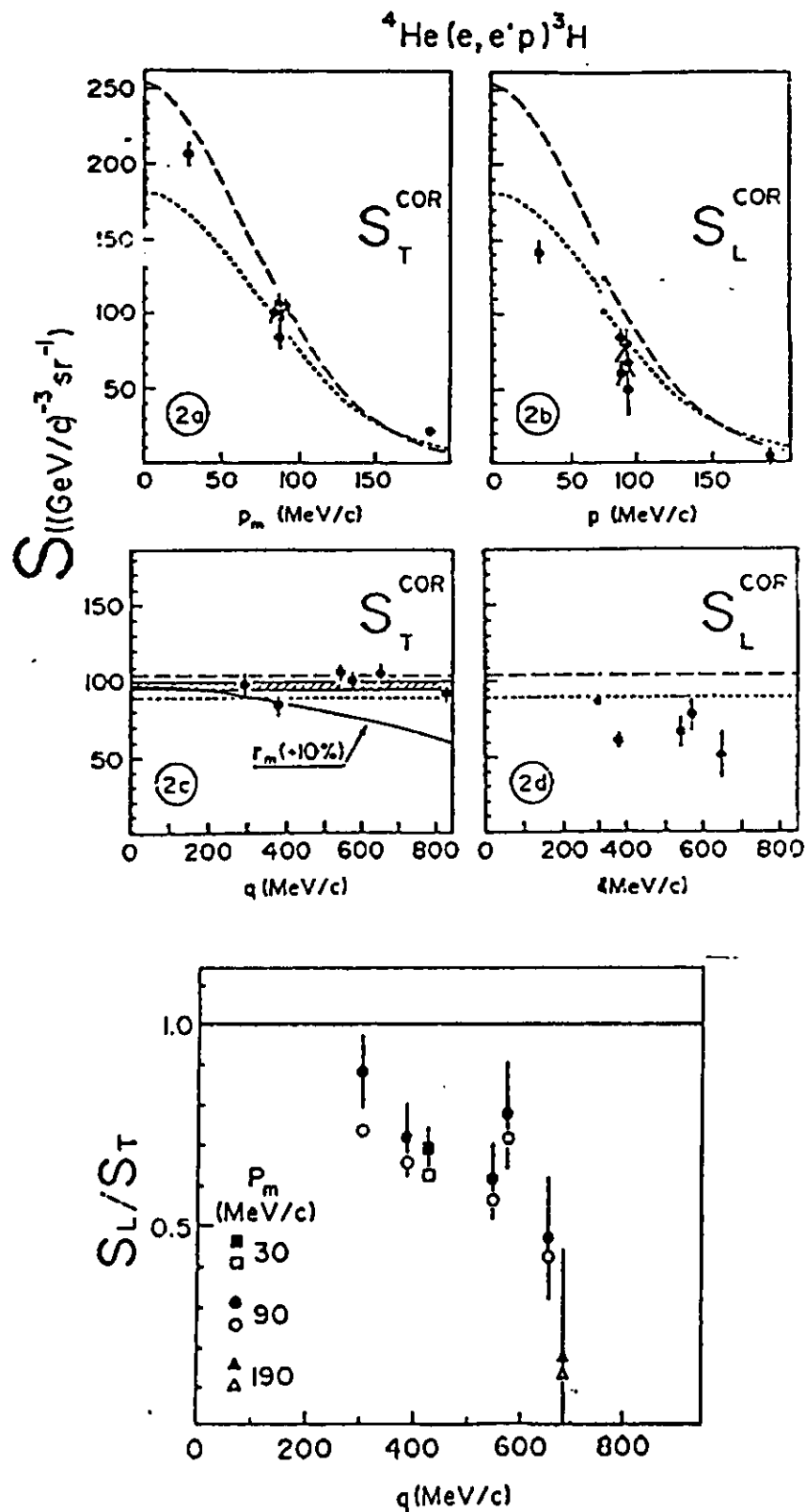
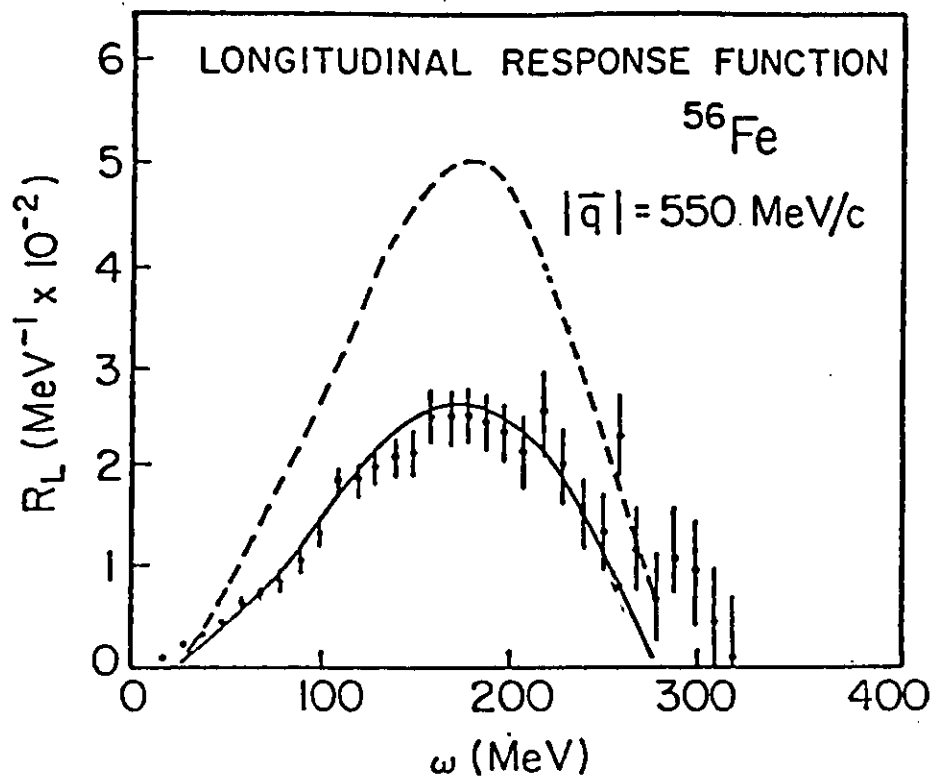
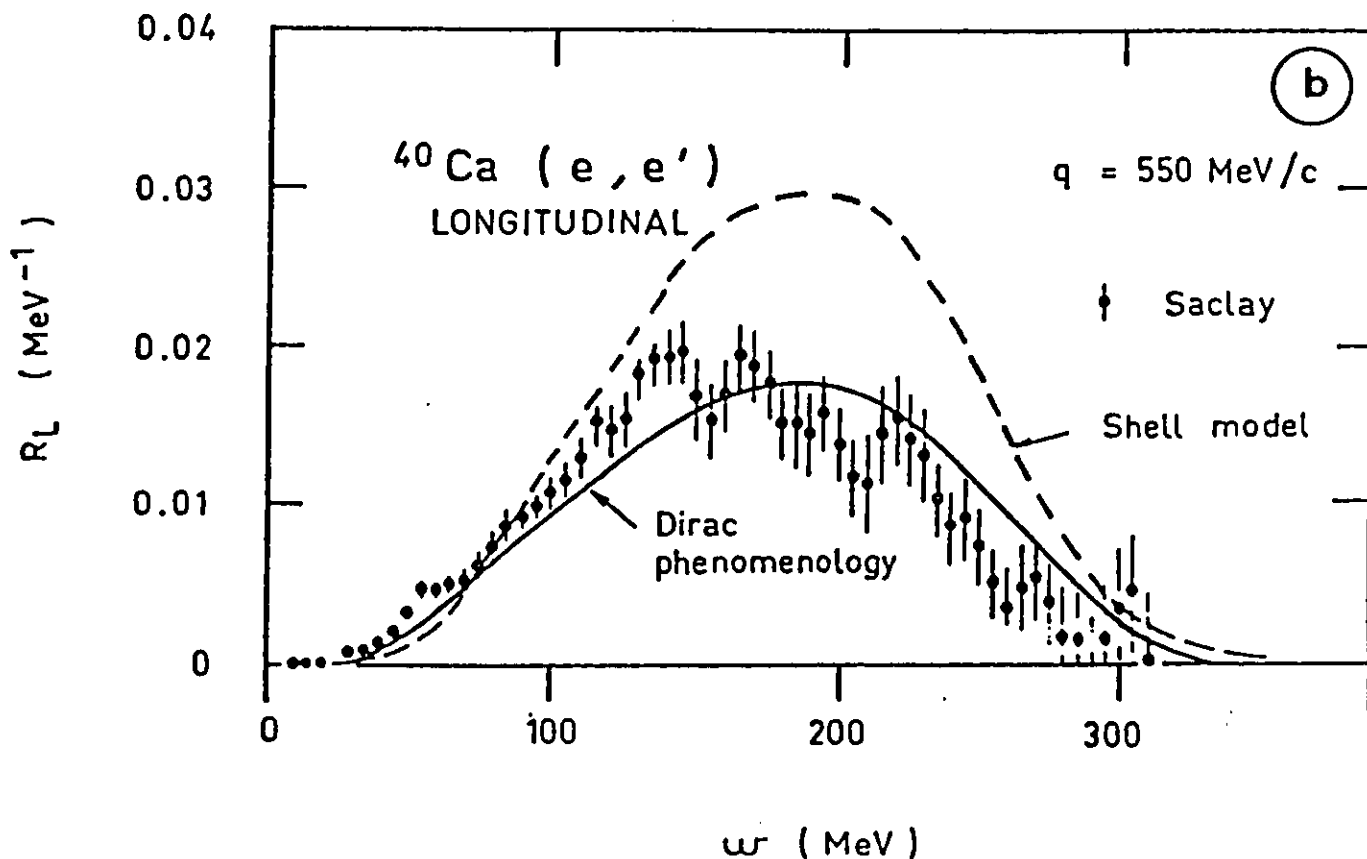


Figure 1. Data corrected for MEC and FSI experimental spectral function, S_T^{COR} (a), and S_L^{COR} (b), shown as functions of missing momentum p_m . Error bars are statistical errors only. The labelled curves assumed different NN potentials. Figs 1c and 1d show S_T^{COR} and S_L^{COR} at constant missing momentum (90 MeV/c) are shown as functions of momentum transfer q . The labelled horizontal lines correspond to the value of the curves in Fig. 1a and 1b at $p_m=90$ MeV/c. Fig. 1e show the ratios of spectral functions; open symbols



(a)



(b)

Figure 2. Saclay data for longitudinal response function of ^{56}Fe and ^{40}Ca at $q = 500 \text{ MeV}/c$. Theoretical curves are from: a) Celenza *et al*, dashed(solid) line using free(modified) nucleon form factors: b) DoDang and Van Giai

Part 3 :Two-Nucleon Correlations

3.1. Physics motivation

The determination of two nucleon densities in nuclei is of fundamental importance. They are a necessary ingredient in the calculation of meson exchange currents, in understanding the high momentum tails of the single nucleon momentum densities as well as in the analysis of the high Q^2 electron scattering data.

The most direct access to two-nucleon density distributions is through two nucleon emission ($e, e'2N$) or ($\gamma, 2N$) reactions. Without entering into the full complexity of a triple coincidence experiment, information on the two-body density can be obtained from the more exclusive ($e, e'N$) reaction under kinematics which favor the absorption of the photon on a nucleon pair. This has been recently demonstrated in an unambiguous way by C. Marchand^[29] in the ${}^3\text{He}(e, e'p)np$ reaction at 560 MeV. Excess of strength at high missing energy in ${}^{12}\text{C}(e, e'p)$ experiments at Bates in the quasielastic,^[24] “dip”^[30] and quasifree Δ -production^[31] regions indicate also important contributions from two-nucleon knock-out processes. Our purpose is to extend the ($e, e'p$) measurements on ${}^3\text{He}$ to higher momentum transfer and higher internal momenta in the initial pair. Higher statistical accuracy and a longitudinal/transverse separation should allow a more quantitative analysis of the process.

Figure 3 shows the data of Marchand et al.^[29] at three different proton angles as a function of the missing energy E_m .

The broad structure above 20 MeV is found to move towards higher E_m values when the recoil momentum p_R increases. The arrows locate the value of $(E_m)_c = p_R^2/4M_p$ which one would obtain assuming that the following process takes place at this point:

- The virtual photon is absorbed on a 2-nucleon pair initially at rest, and the proton of the pair is detected.
- Its partner - most likely a neutron - recoils with \vec{p}_R . The third nucleon stays at rest (spectator).

- The peak width reflects the motion of the center of mass of the pair in the initial nucleus.

The theoretical curves, from a calculation by Laget^[32] along these lines, confirm nicely the above interpretation of the data. We shall come back later on to this calculation, which we have used in our counting rate estimates.

It is worth noticing that, as the recoil momentum increases, the two-nucleon contribution dominates over the “one-body” peak at $E_m = 5.5$ MeV. This clearly shows that high momentum components in nucleon wave functions arise mainly from violent two-nucleon interactions. Indeed, “exact” calculations of the ${}^3\text{He}$ ground-state wave function support this interpretation. Figure 4, from Ciofi degli Atti *et. al.*,^[33] shows proton momentum distributions in ${}^3\text{He}$ obtained by integrating the one-body spectral function $S(\vec{p}, E_m)$

$$n(\vec{p}, E_{max}) = \int_0^{E_{max}} S(\vec{p}, E_m) dE_m \quad (7)$$

One clearly sees that, above $p \sim 400$ MeV/ c , the strength appears almost entirely in the continuum, up to $E_m = 300$ MeV. In this calculation $S(\vec{p}, E)$ has been determined using variational wave functions obtained from the Reid soft core interaction. Faddeev-type calculations lead to similar conclusions.

Up to now, both incident energy and duty cycle have been limiting factors in such studies. With the high energy, high duty cycle beam of CEBAF they can be fully developed, and their results will serve as a basis for more involved triple coincidence studies, the same way single arm quasielastic results triggered more exclusive $(e, e'p)$ experiments. Two main issues can be addressed, and are included in our proposal:

- *Higher momentum transfers and higher internal momenta in the initial pair.* This will enhance both the sensitivity to multinucleon processes versus one-body knock-out, and to very short-range effects. In particular, one should be able to test alternate descriptions of two-nucleon correlated pairs in terms of 6-quark clusters, as already proposed for inclusive (e, e') scattering (see Figure 5 from Ref. [8]). Relativistic effects will have also to be considered.

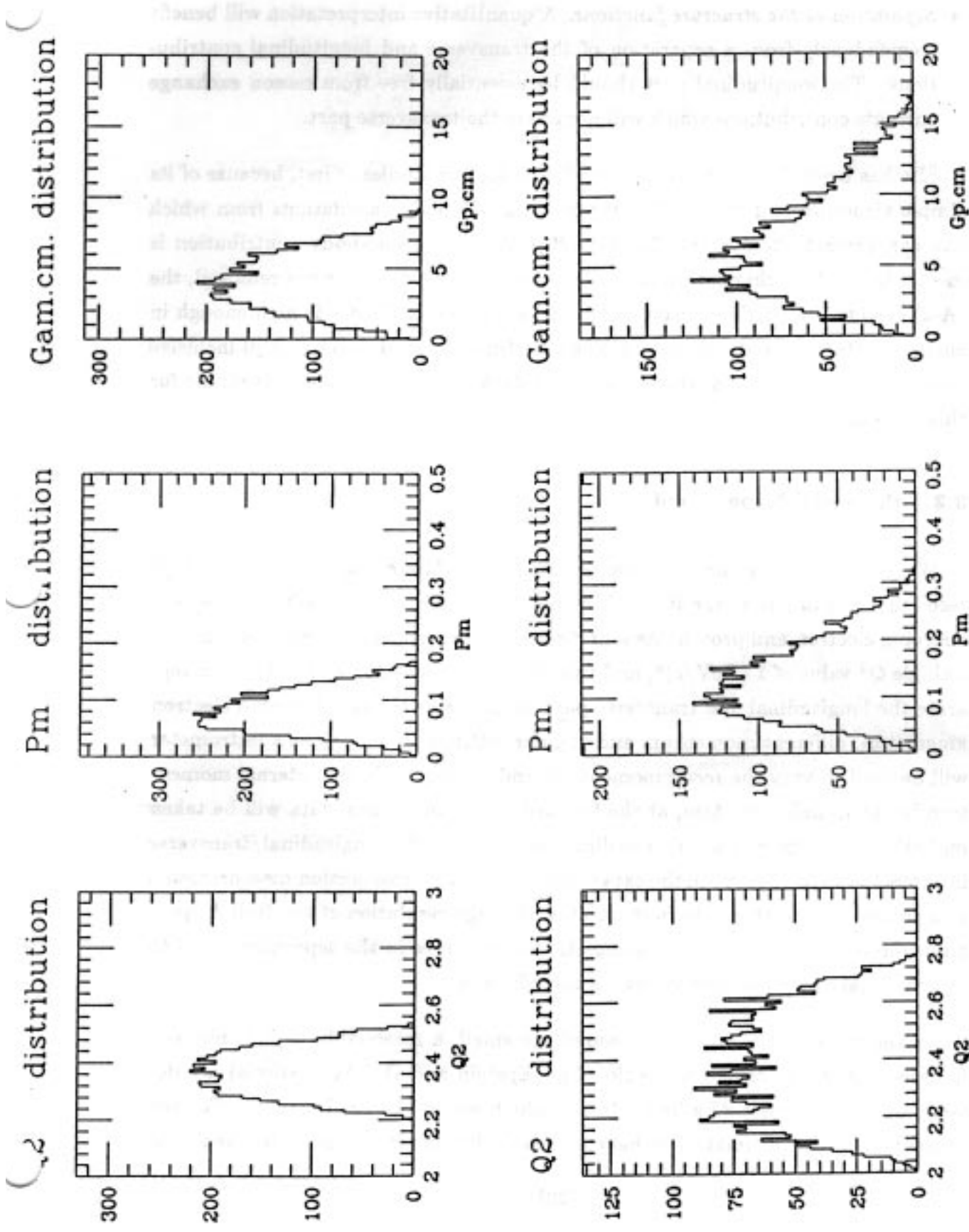


Figure 3. Phase space acceptances for the ${}^3\text{He}(e, e'p)$ reaction with the HRS pair for $q = 2\text{GeV}/c$; the top three histograms are for the forward angle setup and the bottom three are for the backward angle setup.

- *Separation of the structure functions.* A quantitative interpretation will benefit tremendously from a separation of the transverse and longitudinal contributions. The longitudinal part should be essentially free from meson exchange currents contributions which will dominate the transverse part.

^3He has been chosen as the first candidate for our studies. First, because of its simple structure and the availability of “exact” 3-body calculations from which one can extract the spectral function $S(\vec{p}, E_m)$. The one-body contribution is mostly in the (pd) channel which is easily separated. Once a pair is removed, the $(A-2)$ system is a single nucleon, of which the first excited state is high enough in energy not to wash out the two-nucleon structure observed in the $(e, e'p)$ inclusive measurement. Also, a substantial body of data and calculations is available for this nucleus.

3.2. Proposed Experiment

We propose to measure the cross section for the $^3\text{He}(e, e'p)X$ reaction at high recoil momentum, using the Hall A high resolution spectrometer pair to detect the outgoing electron and proton. As a first step, the experiment will be performed at a single Q^2 value of $1 \text{ (GeV}/c)^2$, and two electron angles - 15° and 104.5° - to separate the longitudinal and transverse parts of the cross section. For each electron kinematics, different momentum and angular settings of the proton spectrometer will be used to vary the recoil momentum, and consequently the internal momentum in the initial pair. Also, at the forward angle kinematics, data will be taken on both sides of the virtual photon direction to isolate the longitudinal/transverse interference term. Although the experiment deals with cross section measurements in a continuum with no sharp structures, the high resolution of the Hall A spectrometers is needed to control systematic uncertainties in the separations and to clearly isolate the two body break-up contribution.

As the cross sections to be measured are small, a reasonably high luminosity is necessary. Some of us (A. Aniol, M. Epstein and D. Margaziotis) are developing a high power ^3He liquid target which would be ideally suited. For the present count rate estimates, we have assumed a luminosity of 10^{36} , obtained from

a beam intensity of $10\mu\text{A}$ on a 4 cm diameter gas target operating at 21°K and 15 atm. Although it is likely that we will be able to use much higher luminosities (factor of 5 to 10), more detailed calculations of single rates, accidentals and pion contamination have to be performed before giving any definite value for the luminosity.

3.3. Cross Sections and Counting Rates

Table I gives the kinematics we used to evaluate the counting rates. The quantity p' represents the momentum of the detected proton, θ_{pq} (θ_{cm}) its angle with respect to the virtual photon direction in the laboratory (center of mass) system. The quantity θ_p represents the proton angle with respect to the beam direction. The two-nucleon contribution is expected to peak at $E_m = (E_m)_c$. It corresponds to the "spectator" nucleon being at rest, i. e. the center of mass of the pair being at rest in the initial nucleus, if one considers only the PWIA graph (Figures 1a and 2). Consequently, \vec{p}_R is the momentum of the second partner in the pair, the first one being the detected proton. Two situations may occur: a) the detected proton is the nucleon which absorbed the virtual photon (\vec{p}'_1 of Figure 2). In that case, p_R is equal to the relative momentum p_r of the initial pair (see eq. 4). b) The virtual photon was absorbed by the undetected nucleon, the detected proton being the spectator of the pair (\vec{p}'_2). In that case $p_r = p'$.

The six-fold differential cross section for the $(e, e'p)$ reaction in the continuum is written as

$$\frac{d^6\sigma}{de' d\Omega_e dp' d\Omega_p} = \Gamma_\nu [\sigma_T + \epsilon\sigma_L + \epsilon \cos(2\phi) \sigma_{TT} - \sqrt{\frac{\epsilon(\epsilon+1)}{2}} \frac{Q}{\omega} \sigma_{TL}] \quad (8)$$

where

$$\Gamma_\nu = \frac{\alpha}{2\pi^2} \frac{1}{Q^2} \frac{e'}{e} \frac{|\vec{q}|}{1-\epsilon} \quad (9)$$

is the virtual photon flux. The quantities $\sigma_i = \frac{d\sigma_i}{d\Omega_p dp'}$, are partial cross sections for the photoreaction.

Table Ia

Electron Kinematics							
	e (GeV)	e' (GeV)	θ_e (deg.)	$ \vec{q} $ (GeV/c)	θ_q (deg.)	Q^2 (GeV/c) ²	ϵ
Forward	4.142	3.542	15	1.166	51.8	1	0.955
Backward	1.000	0.400	104.5	1.166	19.4	1	0.181

Table Ib

Proton Kinematics

θ_{cm} (deg.)	p' (GeV/c)	p_R (GeV/c)	$(E_m)_c$ MeV	θ_{pq} (deg.)	Forward		Backward
					$\theta_p^{(2)}$ (deg.)	$\theta_p^{(1)}$ (deg.)	$\theta_p^{(3)}$ (deg.)
30	1.163	0.279	16.1	13.8	38.	65.6	33.2
45	1.093	0.415	46.2	20.8	31.	72.6	40.2
60	1.014	0.549	73.4	28.1	23.7	79.9	47.5
75	0.911	0.679	109.8	35.6	16.2	87.4	55.0
90	0.806	0.802	139.9	43.4	-	95.2	62.8
105	0.686	0.916	173.0	51.7	-	103.5	71.1
120	0.558	1.015	204.6	61.0	-	112.8	80.4

Each line in Table 1b corresponds to three kinematical points: two of them - $\theta_p^{(1)}$ and $\theta_p^{(2)}$ - refer to the forward electron kinematics with $\theta_p > \theta_q$ and $\theta_p < \theta_q$ respectively. The third one, $\theta_p^{(3)}$, refers to the backward kinematics. From the total photoreaction cross section σ (i. e. the bracket in eq. [8]) measured in the three kinematics, the partial cross sections will be extracted as follows:

$$\sigma_T = \frac{(a_F \epsilon_B + a_B \epsilon_F)\sigma_1 + (a_F \epsilon_B - a_B \epsilon_F)\sigma_2 - 2 a_F \epsilon_F \sigma_3}{2 a_F (\epsilon_B - \epsilon_F)} \quad (10)$$

$$\sigma_L + \sigma_{TT} = \frac{-(a_F + a_B)\sigma_1 + (a_B - a_F)\sigma_2 + 2 a_F \sigma_3}{2 a_F (\epsilon_B - \epsilon_F)} \quad (11)$$

$$\sigma_{LT} = \frac{\sigma_1 - \sigma_2}{2 a_F} \quad (12)$$

where

$$a_i = \sqrt{\epsilon_i(\epsilon_i + 1)} \frac{Q}{\omega\sqrt{2}} \quad (13)$$

Note that the separation will only be possible up to $p_R = 0.679$ GeV/c, due to angular interference between the two spectrometers.

The partial cross sections σ_T , σ_L , σ_{TT} and σ_{LT} have been computed by Laget.^[10,11] The calculation includes contributions from final-state interactions between all three nucleons and meson exchange currents. Their relative contributions in the Saclay kinematics are shown in Figure 3 and a sample of them is given in Table

II for our kinematics. The contribution listed under PW refers to the graph of Figure 1a where the nucleon being detected is either the one which absorbed the photon or a spectator one. Note that at $\theta_{pq} = 20.8^\circ$ where $p' \gg p_R$, the PW contribution dominates. In the case of θ_{pq} ($p' < p_R$) however, final state interactions dominate and so they have to be carefully evaluated. Figure 6 shows the missing energy distribution of the photoreaction cross section σ for the two values of the proton-photon angle θ_{pq} given in Table II. Figure 7 gives the total $(e, e'p)$ cross section for the two-nucleon emission contribution integrated over the missing energy. Figure 8 shows the corresponding partial photoreaction cross sections.

Table II

Partial photoreaction cross sections for the ${}^3\text{He}(e, e'p)np$ reaction (from Laget, ref. [11]). The cross sections, in $\text{nb}/(\text{MeV sr})$, are given at $E_m = (E_m)_c$

θ_{pq}		PW	+FSI	+FSI+MEC
20.8°	σ_T	63.43	54.41	83.41
	σ_L	27.67	23.78	23.78
	σ_{TT}	3.92	11.36	1.01
	σ_{TL}	-11.66	-12.97	-16.05
	σ	74.81	67.09	81.24
51.7°	σ_T	0.269	2.76	4.27
	σ_L	0.077	0.770	0.770
	σ_{TT}	0.140	1.12	1.13
	σ_{TL}	0.051	0.75	0.544
	σ	0.558	5.78	6.95

Table III gives the expected counting rates for the kinematics of Table I, together with single electron, single proton and accidental coincidence rates. A 3ns time window is considered, assuming $\sim 1.2\text{ns}$ FWHM time resolution for the e-p coincidence. No cuts have been introduced in the evaluation of the accidentals, although some regions of the (E_m, p_R) acceptance can probably be discarded for the process we are interested in.

From Figure 6 it is clear that, at backward angles, the 10% momentum acceptance of the electron spectrometer will not suffice to cover the desired range in E_m in a single setting.

We used these rates to estimate to which degree of accuracy we would be able to separate the various structure functions. Counting times necessary to reach 0.3% statistical error on the integrated cross section have been considered, however limited to 96 hrs per angle. An optimistic systematic error of 1% has been folded in. The errors on the determination of σ_T , σ_{TL} and the combination $\sigma_L + \sigma_{TT}$ are shown in Figure 9.

Important note

We plan to incorporate in Part 3 some measurements on ^3He in the kinematics proposed in LOI41 by Epstein *et al.* This will be discussed in our presentation to the ^{PAC}~~TAP~~. A copy of LOI41 and a complement on that kinematics is attached to the present proposal.

Table III

 ${}^3\text{He}(e, e'p)np$ counting rates

θ_{cm} (deg.)	θ_e (deg.)	θ_p (deg.)	N_e (sec $^{-1}$)	N_p (sec $^{-1}$)	N_T (hr $^{-1}$)	N_A (hr $^{-1}$)	$\frac{N_T}{N_A}$
30	15	65.6	1800	340	4997	1.9	2600
	15	38.	1800	5700	8177	49.	167
	104.5	33.2	27	24000	39.5	0.64	62
45	15	72.6	1800	270	1602	1.5	1070
	15	31	1800	6600	2748	45.	61
	104.5	40.2	27	24000	15.9	0.63	25
60	15	79.9	1800	280	1095	1.6	680
	15	23.7	1800	7700	1534	43.	36
	104.5	47.5	27	23000	10.4	0.60	17
75	15	87.4	1800	340	699	1.9	370
	15	16.2	1800	8500	1089	47.	23
	104.5	55.0	27	21000	10.3	0.55	19
90	15	95.2	1800	390	454	2.1	220
	104.5	62.8	27	16000	4.7	0.43	11
105	15	103.5	1800	640	274	3.5	78
	104.5	71.1	27	14000	3.9	0.37	11
120	15	112.8	1800	1080	148	6.0	25
	104.5	80.4	27	11000	2.8	0.30	9

NOTE: N_T represents the true coincidences while N_A the accidental coincidences

3.4. Beam Time Request

In view of these counting rates, and assuming that the luminosity can be increased by a factor of 5 - which would bring the true/accidental ratio around 2 in the worst case - we estimate that 300 hours of beam time would be necessary for data taking.

FIGURE CAPTIONS

- Fig. 1. “Direct” two-nucleon emission processes.
- Fig. 2. Two-nucleon emission process in PWIA. Kinematical notations.
- Fig. 3. Missing energy spectra for the ${}^3\text{He}(e, e'p)$ reaction at 560 MeV (from Ref. [2]). Dotted (solid) histograms show data before (after) radiative corrections. Curves are theoretical predictions. Arrows indicate values of $(E_m)_c$ which correspond to the indicated p_R (see text).
- Fig. 4. The proton momentum distribution in ${}^3\text{He}$: (a) two-body break-up; (b), (c) and (d): calculated by integrating $S(\vec{p}, E_m)$ up to $E_{max} = 12.25, 50$ and 300 MeV respectively; (e): total. From Ciofi degli Atti, Ref. [6].
- Fig. 5. Transverse response function for ${}^{12}\text{C}$ at $|\vec{q}| = 400$ MeV/c with the interpretation from Mulders (Ref. [8]) in terms of nucleons and 6-quark clusters. Data are from Ref. [9].
- Fig. 6. Missing energy spectra for the 2-nucleon emission part of the ${}^3\text{He}(e, e'p)$ reaction cross section, at two proton-photon angles in the forward kinematics of Table Ib. Calculation from Laget, ref. [11].
- Fig. 7. Cross section σ_2 and σ_3 from Laget’s calculation, ref. [11] (see text).
- Fig. 8. Partial cross sections $\sigma_T, \sigma_L, \sigma_{TT}$ and σ_{TL} from Laget’s calculation, ref. [11] (see text).
- Fig. 9. Expected uncertainties in the determination of σ_L, σ_T and σ_{LT} . The contribution of σ_{TT} has been neglected.

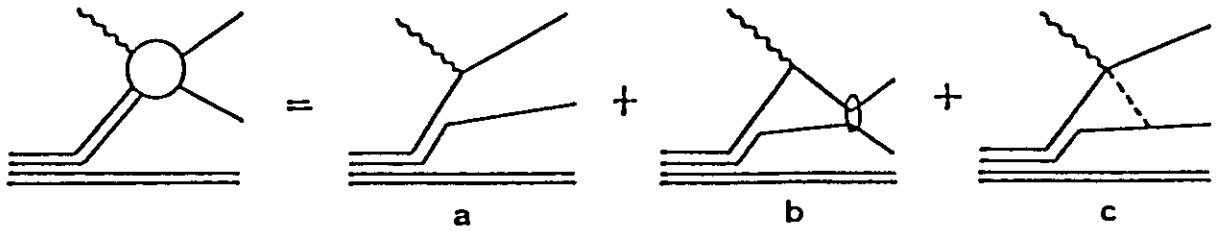


Figure 1

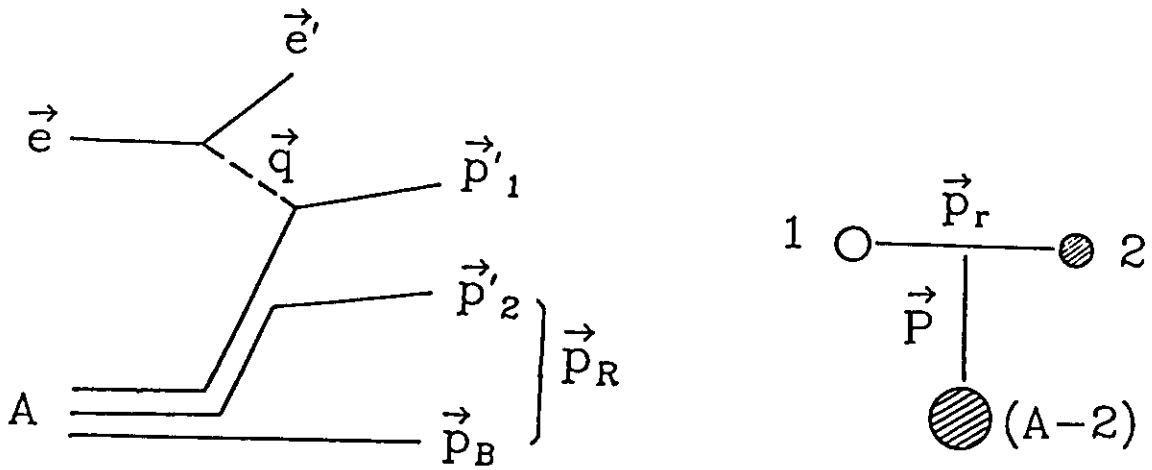


Figure 2

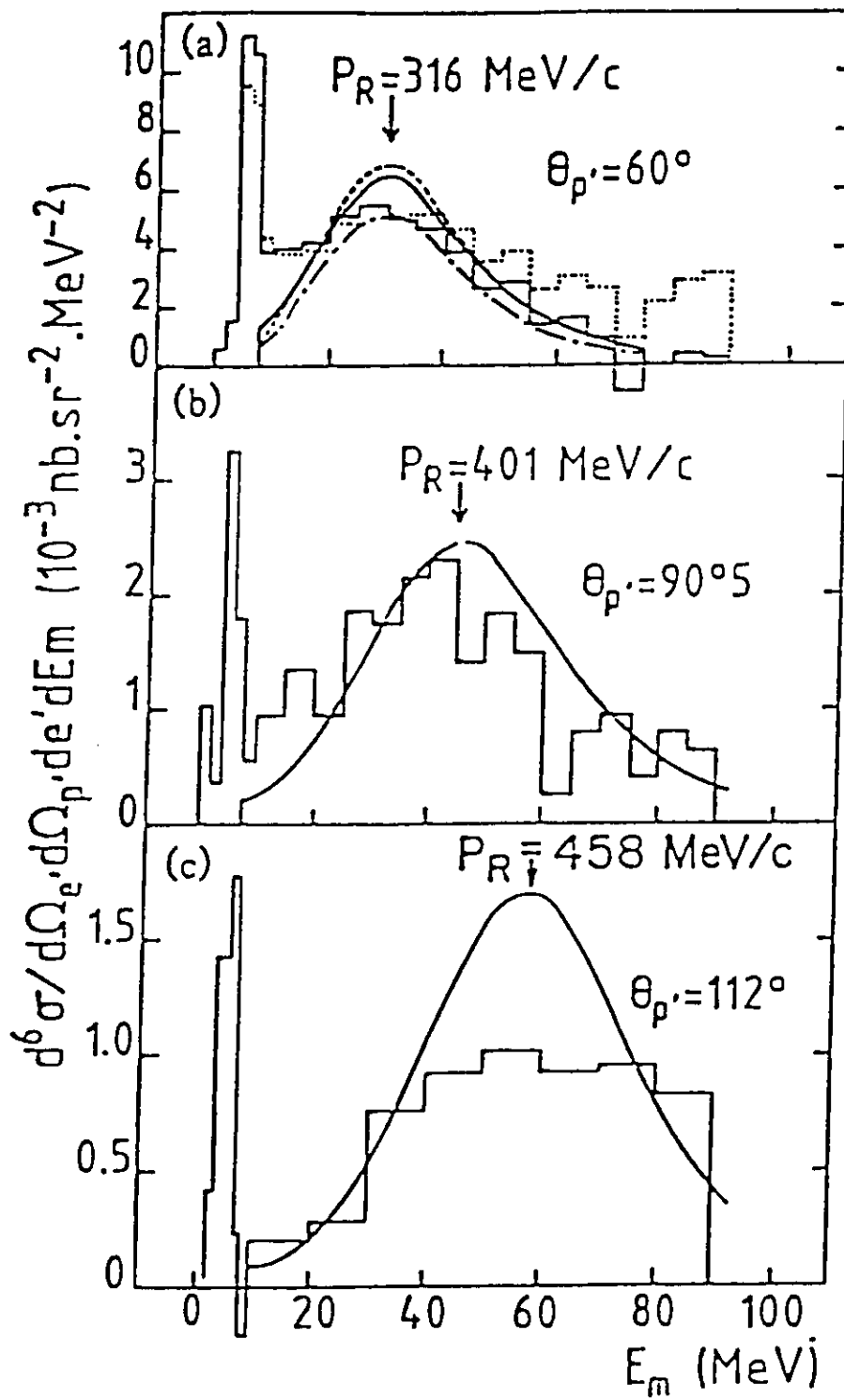


Figure 3

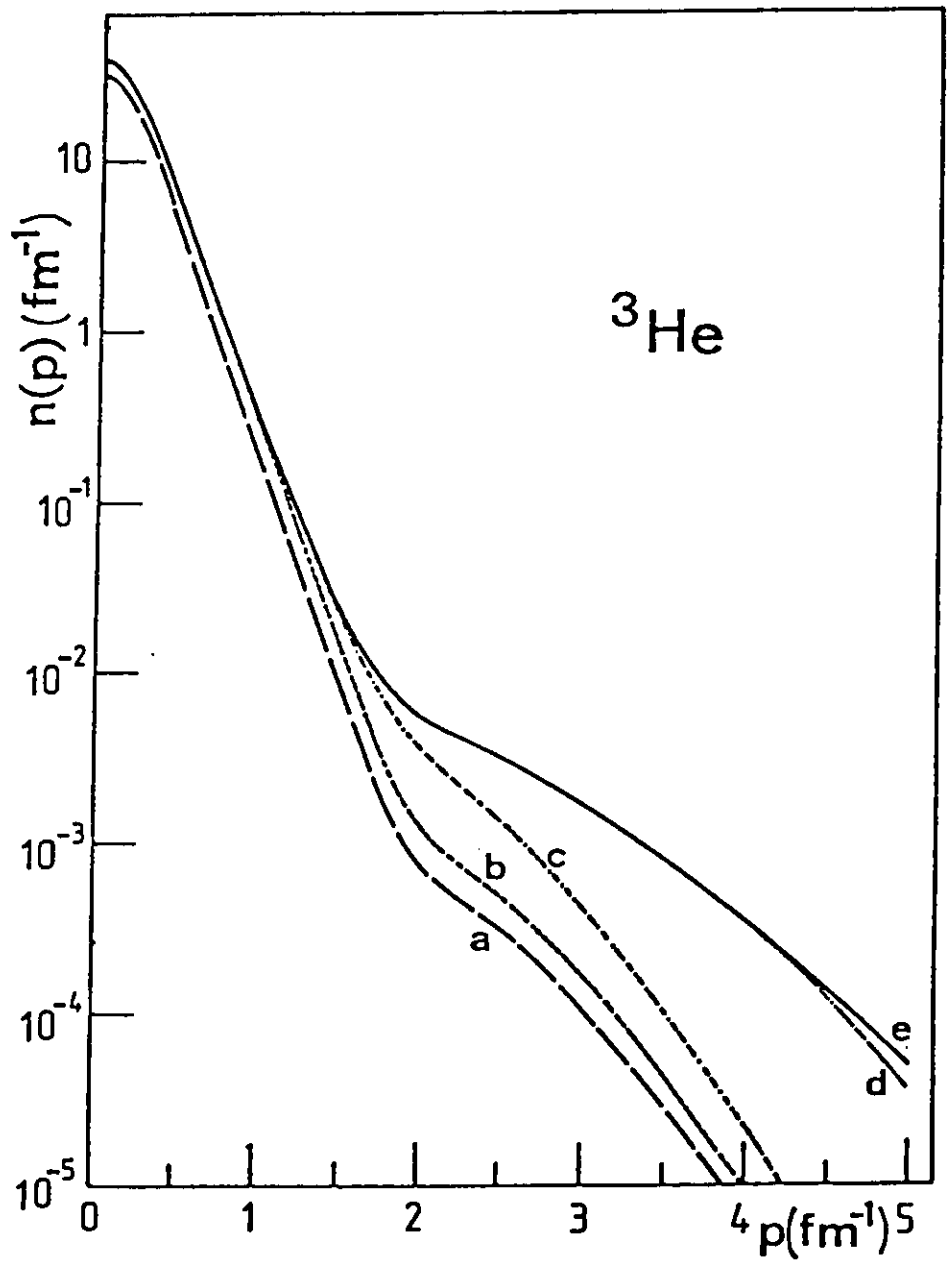


Figure 4

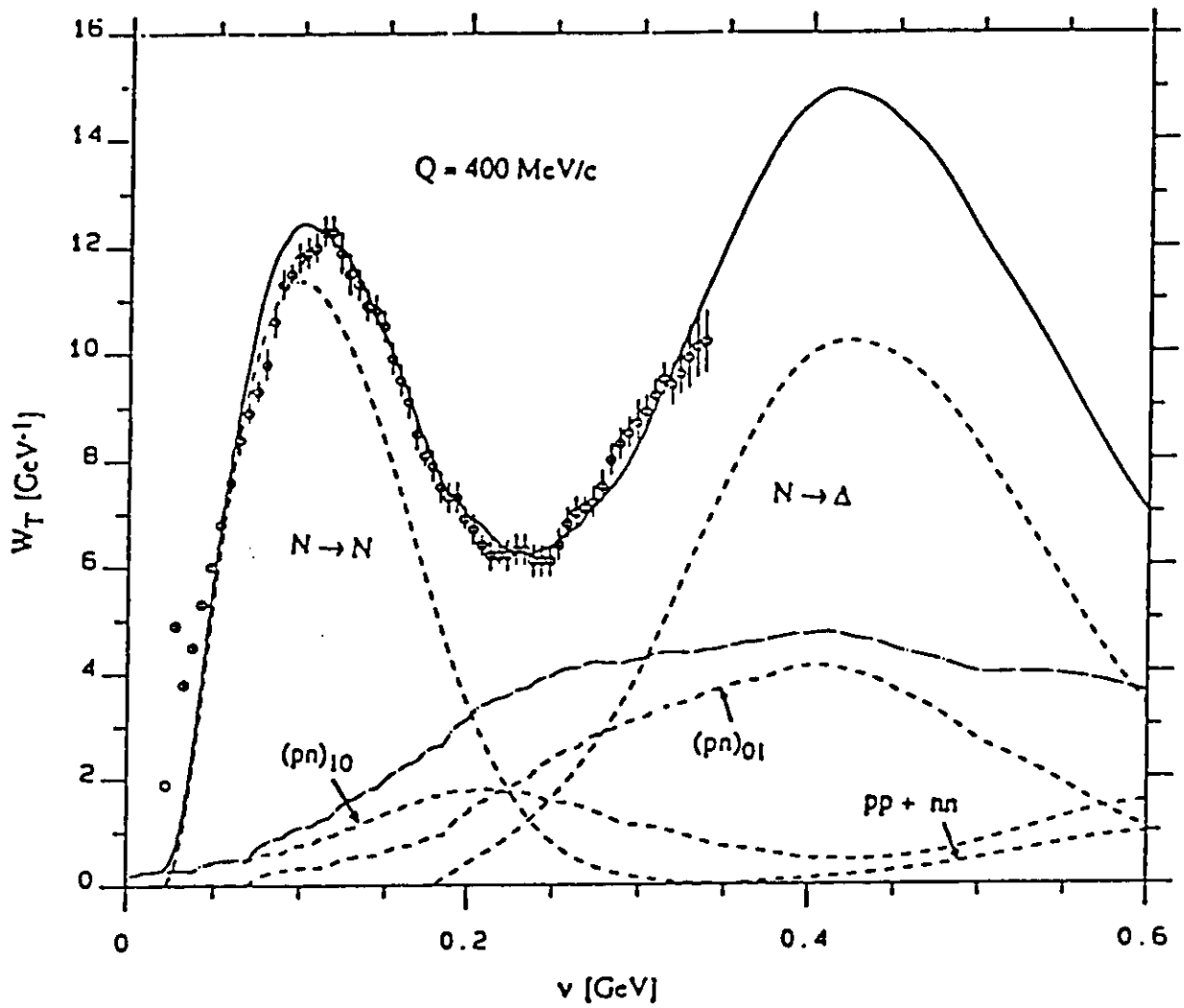


Figure 5

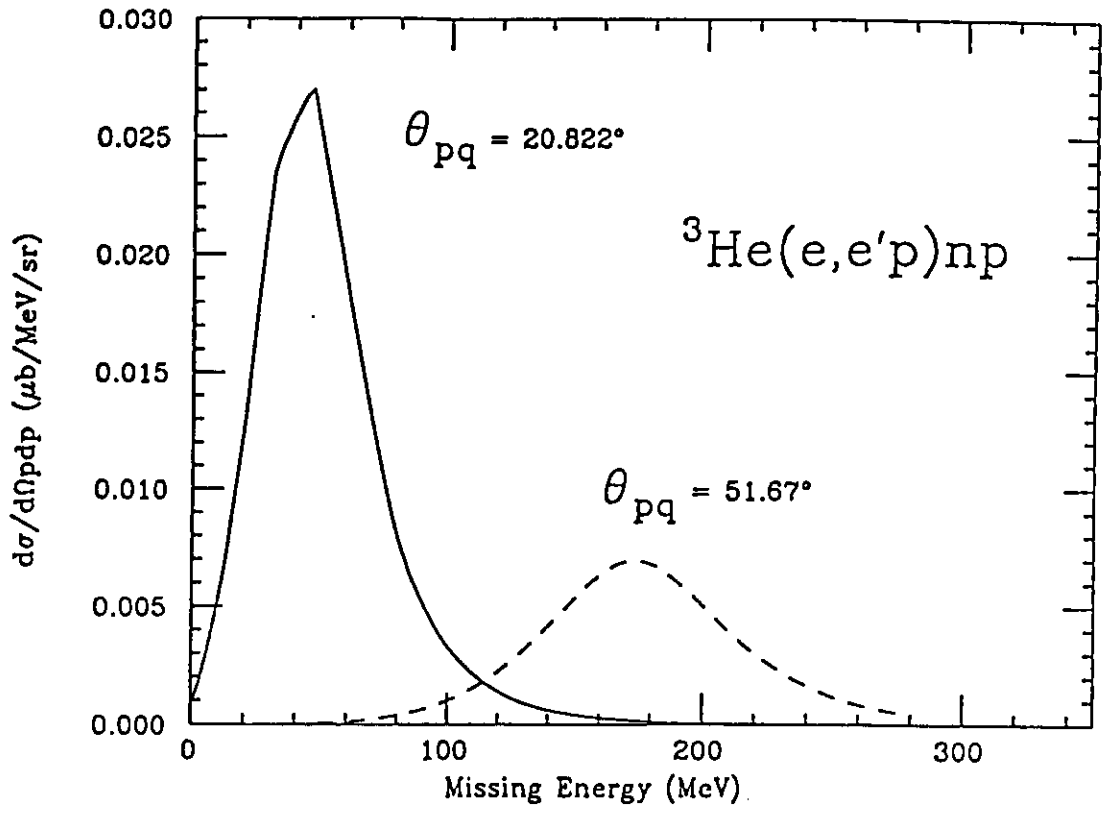


Figure 6

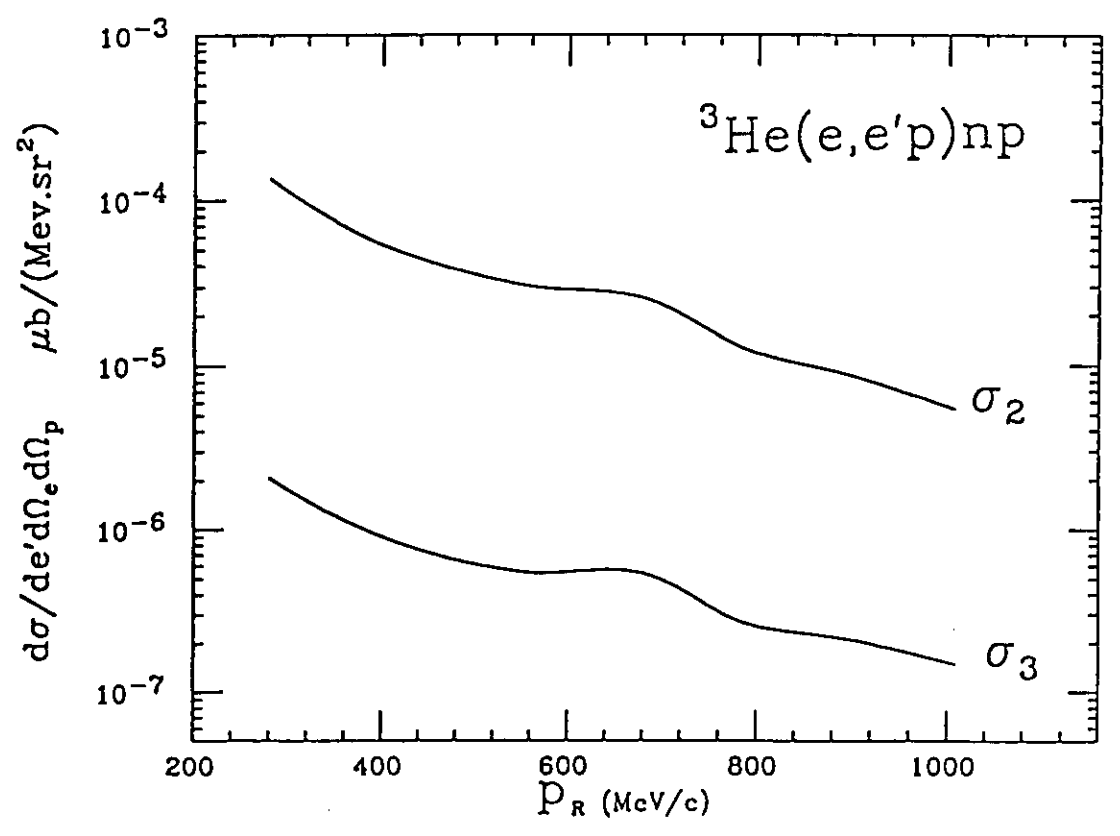


Figure 7

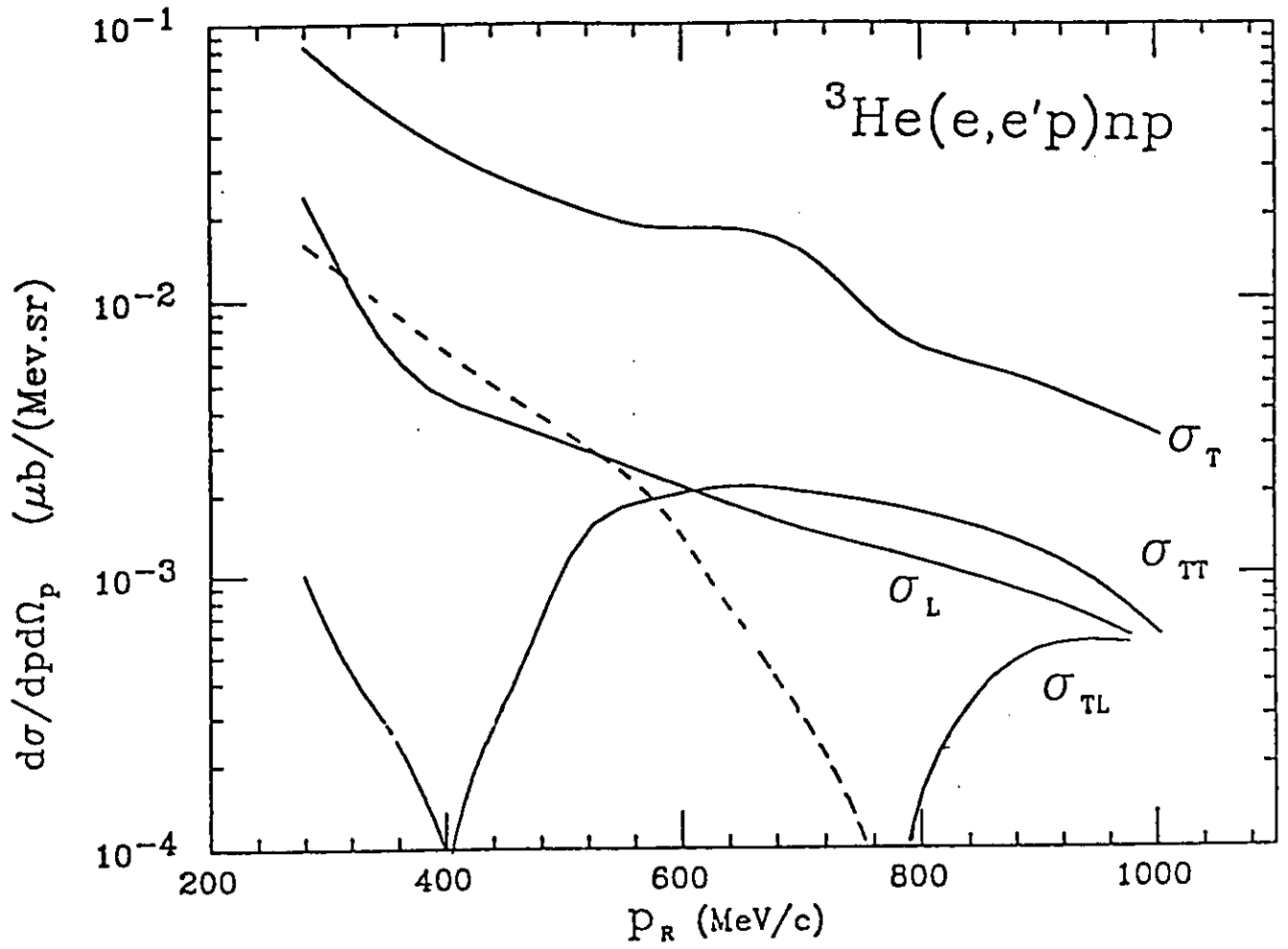


Figure 8

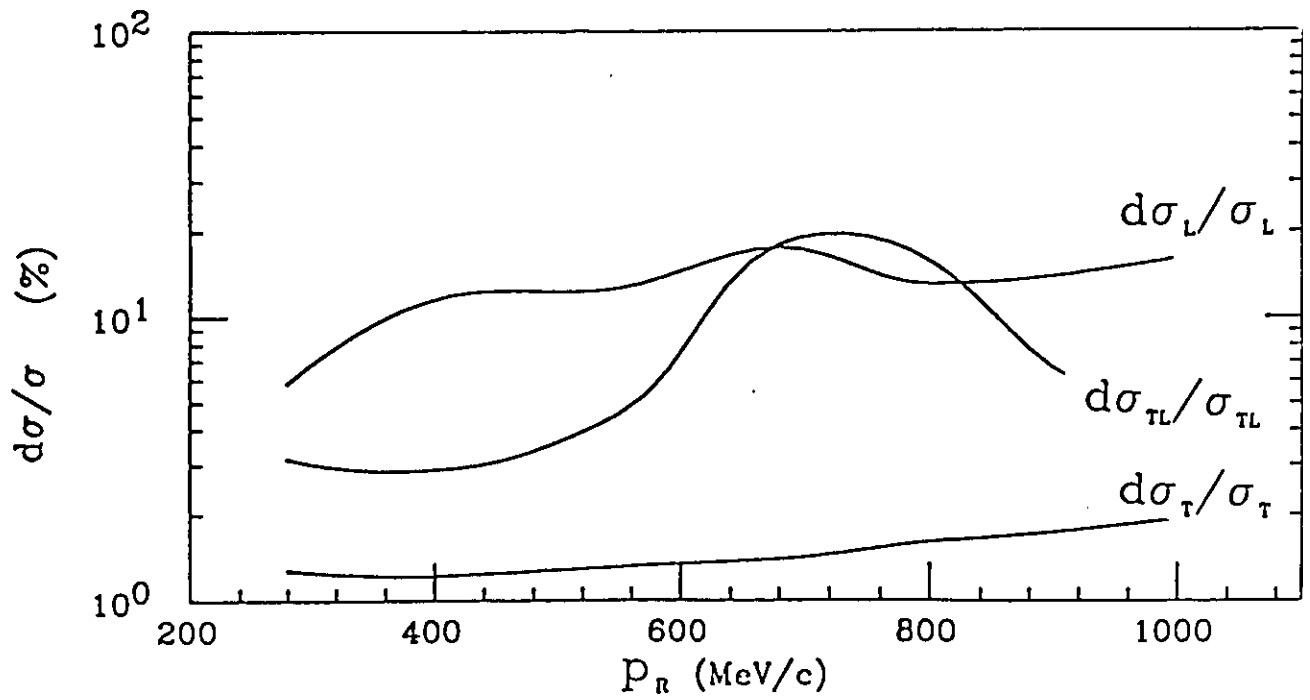


Figure 9

REFERENCES

- [1] R. Schiavilla et al., Nucl. Phys. **A449**, 219 (1988).
- [2] J.M. Laget, Phys. Lett. **B199**, 493 (1987).
- [3] P.H.M. Keizer *et al*, Phys. Lett **197B**, 29 (1987). E. Jans *et al*, Phys. Rev. Lett. **49**, 974 (1982)
- [4] J.F.J. van den Brand *et al*, Phys. Rev. Lett. **60**, 2006
- [5] "(e,e'N) Reactions at CEBAF: A survey of the possibilities with a sample experiment." PAC1 Steering Committee Report, CEBAF, 1987.
- [6] A. Saha and J. Mougey, Research Program at CEBAF, Vol 2, (1987).
- [7] A. Saha, Computer Program HE3EEX.
- [8] P.Ulmer, Computer Program MCEEP.
- [9] T. de Forest, Nucl. Phys. **A392**, 232 (1983).
- [10] H. Meier-Hajduk *et al*, Nucl. Phys. **A395**, 332 (1983).
- [11] J.W. Lightbody and J.S. O'Connell, Computers in Physics **57**, May/June 1988.
- [12] A. Saha, Computer Program EPERP.
- [16] B.D. Serot and J.D. Walecka, *The Relativistic Nuclear Many-Body Problem*, Adv. Nucl. Phys. Vol. 16, Eds. J.W. Negele and E. Vogt, Plenum Press, (1986).
- [17] C. Shakin, Nucl. Phys. **A446**, 323c (1985); J.V.Noble, Phys. Rev. Lett. **46**, 412 (1981).
- [18] S.A. Dytman *et al*, Phys. Rev. **C38**, 800 (1988)
- [19] K. Dow et al. Phys. Rev. Lett. **61**, 1706 (1988)

- [20] C. Marchand *et al*, Phys. Lett. **B153**,29 (1985)
- [21] G. van der Steenhoven *et al*, Nucl. Phys. **A484**, 445 (1988).
- [22] D. Reffay-Pikeroen *et al*, Phys. Rev. Lett. **60**, 776 (1988).
- [23] A. Magnon *et al*, Phys. Lett. **B**, (1989).
- [24] P. E. Ulmer *et al*, Phys. Rev. Lett. **59**, 2259 (1987)
- [25] H.W.L. Naus and J.H. Koch, Phys Rev. **36**, 2459 (1987)
- [26] J. Mougey, Computer Code CARLOUT
- [27] A. Saha and J. Mougey, RPAC III, 1988
- [28] P. E. Ulmer, Computer Code SIGEEP
- [29] C. Marchand *et al*, Phys. Rev. Lett. **60**, 1703 (1988)
- [30] R. W. Lourie *et al*, Phys. Rev. Lett. **56**, 2364 (1986)
- [31] H. Baghaei *et al*, Phys. Rev. **C**
- [32] J. M. Laget, Phys. Lett. **151B**, 325 (1985)
- [33] C. Ciofi degli Atti *et al*, Phys. Lett. **A449**, 219 (1986)

Continuous Electron Beam Accelerator Facility

12000 Jefferson Avenue
Newport News, Virginia 23606
(804) 249-7400

Proposal Number: PR-89-044

Proposal Title: Selected Studies of the ^3He and ^4He Nuclei Through Electrodisintegration at High Momentum Transfer

Spokespersons/Contact Persons: M. Epstein, R. Lourie, J. Mougey, A. Saha

Proposal Status at CEBAF:

Approval for 30 days, for running on ^3He , L/T separations should only be started once the milestone of the 1% accuracy needed for L/T separations has been demonstrated.



John Dirk Walecka
Scientific Director

Updated
Version

Measurement of Two Body Correlations in ^3He and ^3H Via
the $(e,e'N)NN$ Reaction at Zero Recoil

M.B. Epstein, D.J. Margaziotis, and K.A. Aniol

Department of Physics and Astronomy, California State University, Los Angeles

C.F. Perdrisat

Department of Physics, The College of William and Mary

Dej Original
Version State University

ABSTRACT

We propose a series of measurements of the $^3\text{He}(e,e'N)2N$ and $^3\text{H}(e,e'N)2N$ reactions. We will pick particular kinematics that will be sensitive to short range two body correlations. Longitudinal and transverse structure function separations will be done.

Measurements of two body correlations in ^3He and ^3H are of particular interest due to the relative simplicity of the three nucleon wavefunction. In addition three body systems offer particularly simple kinematic situations which allow one to measure the relevant parameters of the final state by measuring only two of the outgoing momenta. We propose exploiting an especially simple kinematic situation that is only available in the three body system.

We will measure the $(e,e'p)pn$ reaction using the two proposed magnetic spectrometers in Hall A, and the $(e,e'n)pp$ reaction using a magnetic spectrometer and a neutron detector. Measuring the momenta of the scattered electron and one of the nucleons in the final state completely determines the center of mass momentum of the recoiling NN pair as well as the relative energy in the center of mass of the NN pair. The proposed measurements will be done for conditions in which the recoiling NN pair is at rest in the laboratory. These conditions are the same as those utilized by Bracco et al. for measurements of the $^3\text{He}(p,2p)pn$ reaction ⁽¹⁾. Under these conditions the magnitudes of the momenta of both of nucleons in the NN pair are determined. In the impulse approximation the incident electron interacts only with the observed nucleon leaving the recoiling NN pair essentially in its initial state condition. In the initial state of the target the relative energy of the nucleons in this pair is directly related to their spatial correlation. A highly correlated pair of nucleons in the target system is confined to a relatively small space and the nucleons in this pair will have a large momentum with respect to the center of mass of the pair. In the impulse approximation this large relative momentum will result in a large final momentum for these nucleons with respect to their center of mass and this of course means a large missing energy for this recoiling pair.

The condition of zero recoil has two advantages. One is that it is particularly restrictive and gives one a relatively unambiguous sampling of the initial state wavefunction. The second is that under the impulse approximation this condition keeps the struck nucleon relatively far from the recoiling pair, since the magnitude of the recoil momentum is just equal to

the magnitude of the initial momentum of the struck proton and this momentum is conjugate to the distance between the NN pair and the struck nucleon. Thus under these conditions one tends to isolate two body correlations from three nucleon interactions.

We note that these kinematics are different from those usually proposed for $(e,e'2N)$ measurements. In our case there is no momentum directly transferred to the NN pair from the virtual photon. Consequently the measurements proposed here should favor a reaction mechanism in which the virtual photon interacts only with the single observed nucleon; whereas the $(e,e'2N)$ case favors a direct interaction with the 2N pair. For the measurements proposed here one samples the entire NN pair for a particular value of relative energy and recoil momentum. That is since we do not directly measure the momentum of the nucleons in the recoiling NN pair we get the yield due to all directions of individual nucleon momenta for this pair. Thus the cross section for this process is intrinsically larger than for the related and more restricted $(e,e'2N)$ measurements. The price one pays is that we do not uniquely determine the relative energy between the struck nucleon and the nucleons in the spectator pair, since the direction of the momenta of the individual nucleons in this pair is not fixed. Consequently the computation for final state interactions is a bit more involved since one has to calculate them for all of the possible relative energies between the struck nucleon and the spectator nucleons. The advantage is that one can do the measurement with only two spectrometers.

We propose a set of related measurements on ${}^3\text{He}$ and ${}^3\text{H}$ using both the $(e,e'p)$ and $(e,e'n)$ reactions for relative NN energies from 0 to at least 200 MeV. The data for the higher relative NN energies should be particularly sensitive to short range two body correlations in the target nuclei. The ${}^3\text{He}(e,e'p)pn$ reaction depends on both $T=0$ and $T=1$ NN components while the ${}^3\text{He}(e,e'n)pp$ is sensitive to only the $T=1$ component. The related reactions on ${}^3\text{H}$ should provide a good check on the neutron detector efficiency. At zero recoil one always is in parallel kinematics and we would also take data to allow a determination of the longitudinal and transverse structure functions. CEBAF will provide the only practical means to make these measurements, particularly for the larger NN relative energies which involve re-

latively small values of the three body spectral function and consequently imply small cross sections.

A sample set of kinematics would be as follows:

1) Incident electron energy = 2838 MeV, electron scattering angle = 15.0° , proton scattering angle = 52.6° , scattered electron energy = 2638 MeV, ejected proton momentum = 795 MeV/c, relative pn energy = 100 MeV, and $Q^2 = -0.47 \text{ (GeV/c)}^2$. (The photon polarization parameter = 0.96)

2) Incident electron energy = 832 MeV, electron scattering angle = 70° , proton scattering angle = 30.7° , and the scattered electron energy = 432 MeV. All the remaining parameters except the photon polarization are the same as in 1). (The photon polarization = 0.43)

Coincidence cross section estimates were made using the plane wave impulse approximation, the ^3He wavefunction of H. Meir-Hajduk et al. ⁽²⁾ and the data of reference 1. Singles cross sections come from the NBS computer codes ⁽³⁾. We have assumed a 10 cm long gas target, solid angles of 8 msr in each spectrometer and energy bites of 10 MeV in each spectrometer. For a luminosity of $2 \times 10^{38} \text{ cm}^{-2}\text{s}^{-1}$ we estimate a real counting rate of 1800 cts/hr for the forward angle data point and 50 counts per hour for the back angle data point. For the forward angle data point the electron singles rates are 20,000 cts/sec and the proton rates are 42,000 cts/sec. For the back angle point one has electron rates of 1000 cts/sec and proton rates of 16,000 cts/sec. This leads to a real to accidental ratio of 0.6 for the forward angle data and 0.7 for the back angle data. If one assumes a resolution along the beam target intersection region of at least 1 cm for each spectrometer then the real to accidental ratio will be improved by at least a factor of 10.

In addition to planning and carrying out these experiments, we are interested in participating, where feasible, in the development of the necessary facilities. This includes the target, neutron detectors, and selected aspects of the magnetic spectrometer systems. We anticipate that the list of collaborators will increase.

REFERENCES

1. A. Bracco, H.P. Gubler, D.K. Hasell, W.T.H. van Oers, M.B. Epstein, D.J. Margaziotis, R. Abegg, C.A. Miller, H. Postma, A.W. Stetz, and P. Schwandt, *Phys. Rev. Lett.*, **50**, 22(1983)
2. H. Meir-Hajduk et al., *Nucl. Phys.* **A395** (1983)332.
3. J.W. Lightbody and J.S. O'Connell, private communication

${}^3\text{He}(e,e'p)pn$

D.J.Margaziotis, K.A. Aniol, M.B. Epstein

October 30, 1989

1 kinematics and count rates

Coincidence cross section estimates were made using the plane wave impulse approximation and the ${}^3\text{He}$ wavefunction of H. Meir-Hajduk et al. ⁽²⁾ (the calculations of Laget shown earlier were used to estimate the contribution of final state interactions for the $E_{pn} = 100$ MeV point only.) Singles cross sections come from the NBS computer codes⁽³⁾. We have assumed a 10 cm long gas target, solid angles of 8 msr in each spectrometer, energy bites of 10 MeV in each spectrometer, and a luminosity of $2 \times 10^{38} \text{cm}^{-2} \text{s}^{-1}$.

2 $E_{pn} = 100$ MeV

For a relative pn energy of 100 MeV the proposed kinematics and count rates are as follows:

1) Incident electron energy = 2837.7 MeV, electron scattering angle = 15.0° , proton scattering angle = 52.6° , scattered electron energy = 2437.7 MeV, ejected proton momentum = 795 MeV/c, relative pn energy = 100 MeV, and $Q^2 = -0.47 (\text{GeV}/c)^2$. (The photon polarization parameter = 0.96)

2) Incident electron energy = 831.1 MeV, electron scattering angle = 70° , proton scattering angle = 30.7° , and the scattered electron energy = 431.1 MeV. All the remaining parameters except the photon polarization are the same as in 1). (The photon polarization = 0.43)

We estimate a real counting rate of 921 cts/hr for the forward angle data point and 35 counts per hour for the back angle data

point. For the forward angle data point the electron singles rates are 19360 cts/sec and the proton rates are 26240 cts/sec. For the back angle point one has electron rates of 1278 cts/sec and proton rates of 16000 cts/sec. This leads to a real to accidental ratio of 0.5 for the forward angle data and 0.5 for the back angle data. If one assumes a resolution along the beam target intersection region of 1 cm for each spectrometer then the real to accidental ratio will be improved by at least a factor of 5, and one should have a real to accidental ratio of 2.5 for both cases.

3 $E_{pn} = 50 \text{ MeV}$

For a relative pn energy of 50 MeV the proposed kinematics and count rates are as follows:

1) Incident electron energy = 3166 MeV, electron scattering angle = 15.0° , proton scattering angle = 55.4° , scattered electron energy = 2766 MeV, ejected proton momentum = 870 MeV/c, relative pn energy = 50 MeV, and $Q^2 = -0.60 \text{ (GeV/c)}^2$. (The photon polarization parameter = 0.96)

2) Incident electron energy = 903 MeV, electron scattering angle = 70° , proton scattering angle = 32.9° , and the scattered electron energy = 503 MeV. All the remaining parameters except the photon polarization are the same as in 1). (The photon polarization = 0.43)

We estimate a real counting rate of 1240 cts/hr for the forward angle data point and 46 counts per hour for the back angle data point. For the forward angle data point the electron singles rates are 28160 cts/sec and the proton rates are 18400 cts/sec. For the back angle point one has electron rates of 1272 cts/sec and proton rates of 4992 cts/sec. This leads to a real to accidental ratio of 0.7 for the forward angle data and 2.0 for the back angle data. If one assumes a resolution along the beam target intersection region of 1 cm for each spectrometer then the real to accidental ratio will be improved by at least a factor of 5, and one should have a real to accidental ratio of 3.5 for the forward angle data and 10 for the back angle data.

4 Beam Time Estimates

For $E_{pn} = 100$ MeV if we require one percent statistics for the forward angle point and three percent for the back angle point we estimate between 40 - 80 hours of beam time is required. (In particular if one uses a pure plane wave impulse approximation estimate for the cross sections then at least 80 hours of beam time is needed, which should probably be doubled to 160 hours to allow for angular cuts etc.)

For $E_{pn} = 50$ MeV if we require one percent statistics for the forward angle point and three percent for the back angle point we estimate about 30 hours of beam time is required which should probably be doubled to 60 hours to allow for angular cuts etc.